Rapid soil degradation following deforestation in Eastern Africa

Laura Summerauer[1,2], Fernando Bamba[3], Bendicto Akoraebirungi[4], Ahurra Wobusobozi[4],
Marijn Bauters[5], Travis W. Drake[1], Negar Haghipour[6,7], Clovis Kabaseke[4], Daniel Muhindo[3], Landry
Cizungu Ntaboba[3], Leonardo Ramirez-Lopez[8,9], Johan Six[1], Daniel Wasner[1], and Sebastian Doetterl[1]

[1]Department of Environmental Systems Science, ETH Zurich, Zurich, Switzerland
[2]Department of Soil Sciences, Research Institute of Organic Agriculture, Frick, Switzerland
[3]Faculty of Agronomy, Université Catholique de Bukavu, Bukavu, Democratic Republic of Congo
[4]Faculty of Agriculture and Environmental sciences, Mountains of the Moon University, Fort Portal, Uganda
[5]Department of Environment, Ghent University, Ghent, Belgium
[6]Department of Earth Sciences, ETH Zurich, Zurich, Switzerland
[7]Laboratory of Ion Beam Physics, ETH Zurich, Zurich, Switzerland
[8]Data Science Department, BUCHI Labortechnik AG, Flawil, Switzerland
[9]Imperial College London, Imperial Business School, London, United Kingdom
Correspondence: Laura Summerauer (laura.summerauer@fibl.org)

Abstract. Deforestation for cropland expansion in tropical sloping landscapes causes severe soil erosion and thus the loss of fertile, organic rich topsoil. The effects of land degradation on tropical soils developed from different parent materials, which may influence soil fertility and soil organic carbon (SOC) content, are still largely unknown. Here, we compared SOC and other soil fertility indicators in undisturbed tropical forest topsoils with cleared hillslope topsoils (cropland, abandoned cropland, and

5   reforestation with *Eucalyptus* monocultures) along the East African rift system using soil chronosequences after deforestation on both mafic and felsic parent material. In the mafic region, we found a consistent decrease of SOC, nitrogen, and phosphorus content with time after deforestation (relative changes of contents up to -69 % SOC, -72 % nitrogen, and -92 % phosphorus). SOC was strongly stabilized by reactive metal phases with little to no benefits to general soil fertility. Consequently, cropland was frequently abandoned by farmers due to the combination of low pH, high Al^{3+} mobility, and low available nutrient status

10   at a relatively high average SOC content of $14–29\,\mathrm{g\,kg^{-1}}$ in topsoils. In the felsic region, mid-Holocene carbonate volcanism mitigated soil degradation to some extent. In both geochemical regions, SOC content did not or only weakly positively correlate with clay content and cation exchange capacity. These results emphasize that soil organic matter, as well as clay content, appear to be unreliable indicators for soil fertility in degraded tropical cropland soils. Additionally, no significant improvement of soil fertility or SOC stocks was observed after replanting degraded fields with *Eucalyptus* monocultures. The estimated lifespan of

15   croplands on hillslopes in our study area, approximately 100–170 years, underscores the severity of soil degradation for food production and forest protection in the upcoming decades, especially considering that many soils are already approaching this age.

1 Introduction

A *civu* turns into a *kalongo*—is the way farmers in South Kivu, Eastern Democratic Republic of Congo, describe the process
when a brown, blackish, and productive soil turns into a degraded, often infertile red soil in their local language, Mashi. Most
subsistence farmers in tropical regions with sloping landscapes are familiar with this process that starts after converting forest
to cropland and the onset of accelerated erosion on farmlands.

The change in color is related to the fact that deforestation and cropland expansion usually lead to a substantial loss of soil
organic carbon (SOC) rich topsoil (Don et al., 2011; Guo and Gifford, 2002; Powers et al., 2011; Veldkamp et al., 2020), which
is black in color compared to the SOC-depleted subsoils, which are red or orange colors that come from the iron minerals.
Compared to other tropical forest ecosystems, deforestation in the Congo Basin has remained low until recently (Rudel et al.,
2009). In the past decades, increasing political instability (Gachuruzi, 1996), agricultural expansion, and the dependency on
charcoal as a primary energy source (May-Tobin et al., 2011; Tyukavina et al., 2018) have led to an acceleration of tropi-
cal forest clearing (Bamwesigye et al., 2022; Depicker et al., 2021; Lambin et al., 2001). Additionally, conflicts in Eastern
Congo, particularly the Congo Wars (1996–2003), significantly impacted agricultural practices and soil fertility by decimating
livestock populations, leading to a substantial reduction in manure application that persists today (Cox, 2012). Alarmingly, a
projected three- to fourfold increase in population by 2100 (Vollset et al., 2020) will likely exacerbate the rate of deforestation
in the coming decades.

Clearing of primary and old-growth forest significantly degrades SOC and fertility. The reduced input of organic matter and
plant nutrients following deforestation (Kurniawan et al., 2018), in combination with changes in microclimate and microbial
communities (Nepstad et al., 1994), leads to higher SOC turnover relative to C input. Moreover, leaching and gaseous emis-
sions decrease the availability of many key nutrients (Klinge et al., 2004; Markewitz et al., 2004; Reichenbach et al., 2023). In
deeply weathered tropical soils nutrient availability primarily depends on new organic matter input (Namirembe et al., 2020)
and atmospheric deposition (Bauters et al., 2018, 2021; Bristow et al., 2010). As a consequence, a sharp decline in soil organic
matter content is often indicative for soil fertility loss (Moebius-Clune et al., 2011) and explains subsequent decreases of crop
yields (Ngoze et al., 2008). SOC content is therefore often used as a proxy for soil fertility, land degradation, and abandonment
(Lal, 2015; Tully et al., 2015).

In addition to reduced OM inputs and microclimate changes, deforestation can also lead to higher rates of soil erosion, which
leads to further losses of SOC and soil fertility (Roose and Barthès, 2001). Along the steep topography of the East African Rift
system, heavy rainfall causes severe soil erosion (Heri-Kazi and Bielders, 2021; Lewis and Nyamulinda, 1996; Wilken et al.,
2021) and landslides (Depicker et al., 2020; Maki Mateso et al., 2023) in deforested areas. Such erosion leads to the loss of
fertile topsoil on hillslopes across many (formerly) fertile soil regions (Muchena et al., 2005). Despite the importance of soil
erosion to soil health and food security (Amundson et al., 2015), our understanding of the timeframe over which it renders

tropical cropland infertile is still limited (Tugel et al., 2005; Xiong et al., 2019).

As erosion progressively removes overlying soil, the surface is brought closer to the underlying saprolite. Hence, less weathered minerals richer in rock-derived nutrients and reactive pedogenic metal phases may become part of the topsoil with the potential to "rejuvenate" soils geochemically (Chadwick and Asner, 2016; Vanacker et al., 2019; Vitousek et al., 2003). The former subsoil nutrients, clays, and reactive metals may therefore increase SOC stocks and soil fertility within the eroding landscape (e.g., Berhe et al., 2007; Stallard, 1998; Van Oost et al., 2012).

If erosion increases the relative exposure of saprolite, the influence of the underlying geochemical composition of the basement rock on SOC and nutrient dynamics can be expected to increase. However, little is known about the interaction of erosion and the mechanisms driving SOC stabilization and soil fertility in tropical soils and whether they differ across geochemical gradients. Indeed, the role of soil mineralogy and soil parent material has often been overlooked in tropical land conversion studies (Powers et al., 2011). Differences in secondary clay minerals and pedogenic metal phases that might promote SOC stabilization, as well as differences between contrasting parent materials, are generally considered to be small in tropical soils. Moreover, it is generally assumed that long-term weathering has homogenized most geochemical distinctions in the tropics (Jenny, 1994; Yavitt, 2000). Recent work, however, illustrates that the geochemistry of soils developed on different parent material can affect soil fertility and the C cycle (Augusto et al., 2017; Bukombe et al., 2022; Doetterl et al., 2018; Reichenbach et al., 2023), even in deeply weathered soils. For example, soils developed from mafic parent material contain more base cations, aluminum (Al), and iron (Fe) than soils developed from felsic parent material with high silica (Si) content (Blume et al., 2016). Thus, soils originating from mafic rocks contain more minerals that help stabilize organic matter. On the other hand, soils formed from felsic mineralogies tend to contain less rock-derived metals (Doetterl et al., 2021a; Reichenbach et al., 2021).

Beyond deforestation, erosion, and soil parent material, land management practices such as reforestation also have the potential to significantly influence SOC and nutrient dynamics in tropical soils. On deforested, eroding, and degraded croplands, instead of abandoning land, farmers sometimes plant tree monocultures such as fast growing *Eucalyptus* varieties (for example in South Kivu; Kangela Matazi et al. (2023)). *Eucalyptus* tolerates poor fertility conditions (Eufrade Junior et al., 2016) and can thus still provide income sources to farmers via timber and charcoal production. However, *Eucalyptus* reforestation has a mixed and inconsistent impact on SOC storage (Laganière et al., 2010; Wells et al., 2023). Further negative effects have been reported, such as acidification and increased Al^{3+} mobility (Jobbágy and Jackson, 2003; Leite et al., 2010; Prosser et al., 1993; Tererai et al., 2015) and nutrient depletion (Guedes et al., 2016; Mallen-Cooper et al., 2022). It is widely unknown whether *Eucalyptus* provides protection against water erosion (Jagger and Pender, 2003) in Eastern Africa and can therefore increase SOC and soil fertility on eroding hillslopes.

Here, we studied how soil degradation affects SOC stocks and fertility in tropical agricultural systems on contrasting geologies. Secondly, we investigated whether SOC stocks and soil fertility recovered after land abandonment or establishing

Eucalyptus monocultures. To accomplish this, we sampled hillslope topsoils in i) two regions with geochemically contrasting parent material (mafic and felsic), ii) along a deforestation chronosequence (0, 2–7, 10–20, 40–60, >60 years), and iii) under different land uses (old growth forest, cropland, abandoned, *Eucalyptus* monoculture). Our working hypotheses were as follows:

1. Hillslope SOC and soil fertility decrease continuously with time after deforestation due to the loss of fertile topsoil through water erosion.

2. We expect that soils developed from mafic parent material can stabilize more SOC than those developed from felsic parent material due to higher amounts of clay and reactive, pedogenic metal phases.

3. Time until cropland abandonment (i.e. soil lifespan) depends strongly on the parent material. Volcanic ash input will delay abandonment due to higher pH (counteracting Al toxicity) and higher soil fertility levels.

4. Reforestation efforts through planting *Eucalyptus* monocultures will increase SOC on degraded soils due to the increased input of organic matter and the reduction of soil erosion. This erosion control prevails over the reported negative effects on soil acidification and nutrient depletion caused in such plantations.

2 Material and Methods

2.1 Site description

We selected two study regions along the Albertine rift (Figure 1). Within each region, sites followed gradients of topography and land cover change, under similar climate but on contrasting soil parent material. The mafic region was located in the eastern Democratic Republic of Congo (DRC; further called "mafic region"), where Late Miocene and Pliocene basalt deposits of volcanoes along the Mitumba mountain chain (10–2.6 Ma, (Kampunzu et al., 1998; Laghmouch et al., 2018; Pouclet et al., 2016)) and in the Virunga volcano area north of the city Goma (Pouclet and Bram, 2021) formed soil parent material with mafic geochemical features (high contents in aluminum, iron, rock-derived base cations and phosphorus (P); Doetterl et al. (2021a)). west of the city of Bukavu with a latitude and longitude range of -2.1– -2.6 and 28.6–28.9, respectively, and at elevations between 1360 to 2250 m.a.s.l. Cropland dominates the lower altitudes and old-growth forest the higher altitudes. The felsic region was located in western Uganda (further called "felsic region"). In this region, soil parent material is primarily composed of felsic magmatic and metamorphic rocks (silica rich, gneissic granites; Doetterl et al. (2021a)) around the city of Fort Portal, in Rwenzori mountain foothills, Itwara and Matiri forest reserves and in Kibale National Park (Link et al., 2010). Mid-Holocene carbonate volcanism had occurred about 4700–5000 b.p.; (Delcamp et al., 2019; Vinogradov, 1980). The study sites in the felsic region are located at latitudes of 0.5–0.8, longitudes of 30.1–30.9, and altitudes of 1230–1760 m.a.s.l. (Figure 1).

Mean annual precipitation (MAP) in the mafic region is 1700 mm, with a rainy season from September to May and a dry season from June to August; mean annual temperature (MAT) is 17.5 °C. In the felsic region, MAP is 1300 mm and MAT

is 20.4 °C (Fick and Hijmans, 2017). In the mafic region, soils are classified as Ferralsols and Acrisols. Nitisols, Phaeozems, Acrisols, and Luvisols dominate the felsic region (Jones et al., 2013). Numerous studies have analyzed volcanic materials
120 from the Fort Portal region and found significant concentrations of primary minerals (e.g., Barker and Nixon, 1989; Bailey et al., 2005; Delcamp et al., 2019). In the felsic cropland sites in the Rwenzori foothills, we measured an average $Al_p : Al_o$ ratio of 0.17 and an average pH value of 5.3 which is an indication for Al present in allophanes (Mizota and Reeuwijk, 1989; López-Ulloa et al., 2005). More detailed information on soil coverage and soil properties in the region can be found in Doetterl et al. (2021a). The topography of both regions is dominated by hillslopes with gentle to steep inclinations (mafic: 10–35 °,
125 felsic: 9–24 °; Table 1). This steep topography causes soil erosion and landslides (Depicker et al., 2021; Jacobs et al., 2017). In both regions, hillslopes which were cleared >60 years ago showed yellowish to red colors of the iron oxides (e.g. goethite and hematite) and the dark topsoils were completely absent. Recently cleared sites were often characterized by remnant burnt tree trunks and charcoal particles. Note that also forest seedlings were still growing between the crops.

130 The main crops in both regions were cassava and maize, with smaller quantities of beans, sorghum, potatoes, groundnuts, coffee, onions, and amaranth. In the felsic region, all visited cropland sites were actively cropped. Here, crops still provide adequate sufficient yields (maize yields: 2–2.5 $\mathrm{t\,ha^{-1}\,yr^{-1}}$ in the Rwenzori foothills in western Uganda (Authority, 2020)). In contrast, in the mafic region, crops perform poorly (maize yields: 0.8–2.1 $\mathrm{t\,ha^{-1}\,yr^{-1}}$ in Walungu, Kabare and Kalehe territories of South Kivu (Mutegeza Mushitwala, 2020)). Consequently, numerous hillslopes in the mafic region were abandoned
135 from cropping due to infertility (information from farmers). A common practice in the mafic region is to plant *Eucalyptus* on heavily degraded hillslopes. In the felsic region *Eucalyptus* plantations are planted regardless of soil status in order to provide fuel for tea plantations. *Eucalyptus* in both regions were grown in monocultures, and sometimes grass, sedges, and rushes grew between the trees. The most common *Eucalyptus* species (family *Myrtaceae*, genus *Eucalyptus*) which are grown in the region are *Eucalyptus globulus*, *Eucalyptus cinerea*, and *Eucalyptus grandis*. For simplicity, we will refer to the genus name
140 *Eucalyptus* only. Abandoned sites were either bare soil or covered with grasses and shrubland vegetation.

2.2 Historical land use

To assess years since deforestation of old-growth or pristine forest (on all cleared hillslope sites, i.e. cropland, abandoned, and *Eucalyptus*), we used a combination of historical aerial imagery and Landsat products. For the mafic region we used
145 the historical, panchromatic aerial photographs from 1955–1958 from the Royal Museum for Central Africa in Belgium. For the felsic region, aerial images from the years 1955–1961 were purchased at the National Collection of Aerial Photography (NCAP). For the years after 1960, satellite-derived Landsat imagery, which is available for Eastern Africa starting from the 80s (Landsat 4–8), historical imagery from Google Earth Pro (Version 7.3.5, last access: 2023-10-12) and the deforestation maps by Hansen et al. (2013) were combined to visually determine years since deforestation for the period 1955–2020 for all sampling
150 locations. This approach allowed us to generate five classes: (1) undisturbed forest (old-growth or pristine forest; also labeled as 0 years since deforestation), as well as altered sites (cropland, abandoned sites, *Eucalyptus* monocultures) at (2) 2–7 years,
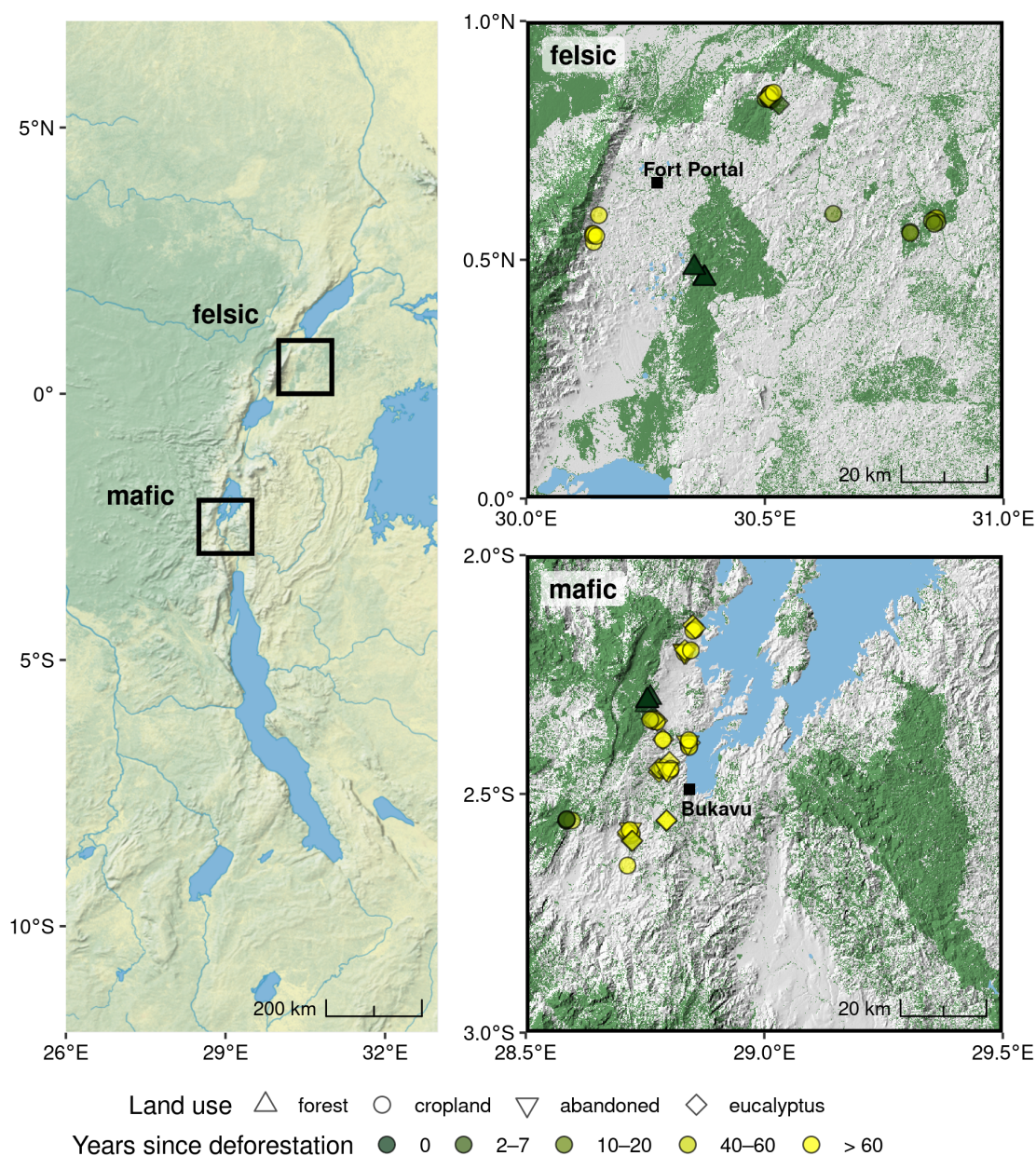
Figure 1. Left: Overview of the Albertine Rift of central Africa with the two sampling regions, mafic and felsic, shown within black boxes. **Right top**: zoomed in view of the felsic region in western Uganda near the city of Fort Portal. **Right bottom**: zoomed in view of the mafic region of South Kivu, Democratic Republic of Congo, west of the city of Bukavu. Sampling sites are marked by their land uses: forest (triangles), cropland (circles), *Eucalyptus* (diamonds), abandoned cropland (upside down triangles). The green to yellow color gradient corresponds to the deforestation chronosequence (0, 2–7, 10–20, 40–60, >60 years since deforestation). Dark green raster color in the right panels indicates forest cover and gray color shows the underlying topography generated from a digital elevation model (source: Natural Earth, SRTM 90 m, ESA CCI 20 m Land Cover map of Africa 2016, HydroLakes)

(3) 10–20 years, (4) 40–60 years, and (5) >60 years sice deforestation. Due to the low temporal coverage and raster resolution of the available satellite imagery, time of planting, harvesting, and replanting of *Eucalyptus* could not be assessed. In summary, in the mafic region we sampled a total of 60 sites with 9 forest sites, 27 cropland sites, 6 abandoned and 18 *Eucalyptus* sites

155 (Table 1). In the felsic region, we sampled a total of 38 sites with 9 forest sites, 26 cropland sites, and 3 *Eucalyptus* sites (Table 1). The different number of sampling sites between both regions stems from difficulties to find abandoned sites in the felsic region.

2.3 Soil sampling and processing

2.3.1 Cropland, *Eucalyptus*, abandoned hillslope sites

160 Eighty samples were collected from hillslopes (cropland: $n = 53$, *Eucalyptus*: $n = 21$, abandoned: $n = 6$) across both geochemical regions along deforestation chronosequences (Figure 1, Table 1). We avoided sampling close to anthropogenic influence other than agriculture (e.g. urban areas, houses, clay mining, and charcoal production). Similarly, we sampled at least $10\,\mathrm{m}$ away from trails and field boundaries. We sampled in four corners of $10 \times 10\,\mathrm{m}^2$ squares on the shoulder to backslope positions of the hillslopes, aiming to effectively capture the spatial variability on a hillslope. Soils were sampled in 0–$30\,\mathrm{cm}$ depth in

165 $10\,\mathrm{cm}$ increments using a sampling ring kit with stainless steel sampling cylinders with a volume of $100\,\mathrm{cm}^3$ (Ejikelkamp, The Netherlands). From the volume-correct samples of each plot we created one composite for each study site and each $10\,\mathrm{cm}$ increment out of 8 samples (2 depths / 0–$5\,\mathrm{cm}$ and 5–$10\,\mathrm{cm}$ times 4 corner locations).

2.3.2 Old-growth and pristine forests

Reference data from undisturbed sites under forest were retrieved from the openly available Tropical Soil Organic Carbon

170 (TropSOC) database v.1.1 (Doetterl et al., 2021a, b). Eighteen forest profiles from plateau and hillslope positions were selected from old-growth and pristine forests in Kahuzi-Biéga National Park in Eastern DRC ($n = 9$) and in Kibale National Park, western Uganda ($n = 9$). Each $1\,\mathrm{m}$ profile consists of composites of $10\,\mathrm{cm}$ increments from four cores, which were taken in a $20 \times 20\,\mathrm{m}^2$ square. Detailed information regarding the sampling and the data is found in Doetterl et al. (2021a). Data compatibility is described in the supplementary material (Appendix B).

175 ### 2.3.3 Vertical transects (soil to bedrock)

To assess soil properties in subsoils down to the saprolite or if possible down to the bedrock parent material, several soil profiles along roadcuts and mines were sampled (felsic: $n = 4$, mafic: $n = 1$) to represent soil development in the two geochemical regions. The soil surface of all profiles was cleaned before each soil horizon was sampled separately. In the mafic region, the saprolite layer started at $530\,\mathrm{cm}$ below surface and the bedrock appeared after $890\,\mathrm{cm}$. In the felsic region, the four sampled

180 road cuts had a maximum depth of 200–$572\,\mathrm{cm}$, the saprolite layer was sampled below $200\,\mathrm{cm}$ depth, and the bedrock was below the sampled profile.

2.3.4 Sample processing

All soil samples from hillslopes, forest, and transects were carefully mixed and oven dried at $40\,^{\circ}$ C and then gently crushed to separate fine soil (<2 mm) from coarse soil (>2 mm) fragments. Soil bulk density was assessed on <2mm sieved soil fraction and used for calculation of SOC stocks. An aliquot of the fine soil of each sample was powder grinded for use in spectroscopic and chemical analyses. All samples from roadcuts or mines below the saprolite boundary were excluded from sieving.

Table 1. Number of sampling sites (n) and inclination (slope °) of the sampled hillslopes under mafic and felsic parent material, under cropland, and forest along the chronosequence of deforestation. Data from forest sites was retrieved from TropSOC database v1.1 (Doetterl et al., 2021a, b)

Land use	Topographic position	Years since deforestation	n	Slope °
		mafic		
forest	plateau, slope	0	9	2–31
cropland	slope	2–7	3	23–29
		10–20	1	18
		40–60	4	11–32
		>60	19	12–30
abandoned	slope	>60	6	15–35
eucalyptus	slope	40–60	5	10–32
		>60	13	14–35
		felsic		
forest	plateau, slope	0	9	2–29
cropland	slope	2–7	3	16
		10–20	13	9–23
		40–60	2	8–15
		>60	5	15–24
eucalyptus	slope	2–7	2	18–19
		>60	1	20

2.4 Soil analyses

2.4.1 SOC, TN, pH_{CaCl_2}, exchangeable cations, and reactive metals

Infrared spectroscopy was used to support the quantification of the key physico-chemical soil variables, namely SOC, total
190   nitrogen (TN), pH_{CaCl_2}, effective cation exchange capacity (ECEC), sum of bases, and reactive metal phases (pyrophosphate and oxalate extractable iron (Fe_{Py}, Fe_{Ox}), and aluminum (Al_{Py}, Al_{Ox}). Together with the present study samples, we also calibrated samples from another ongoing study on soil colluvia with soil cores in one to three meters depth in the same study area. These two sample sets contain a total amount of 1731 individual soil samples from 183 soil cores from the study area. Details on data acquisition, spectral pre-processing, calibration sampling, reference analyses, calibration modeling, and the model validation
195   results are described in the supplementary material (Appendix A and Table A1).

2.4.2 Radiocarbon

Radiocarbon age (^{14}C) and plant available P (P_{resin}) were measured directly and not estimated via MIR spectroscopy, since prior work has illustrated the limitations of spectroscopy to estimate radioisotopic concentrations as well as smaller, labile fractions of C, N and P in soil solution (Doetterl et al., 2021a; Ng et al., 2022; Sanderman et al., 2020). ^{14}C was measured on
200   13 hillslope cropland topsoils cleared >60 years ago (mafic: $n = 8$, felsic: $n = 5$), as well as three subsoil samples, two under cropland (10–20 cm and 20–30 cm), and one under *Eucalyptus* (20–30 cm). This was done to estimate the relative contribution of modern carbon in degraded topsoils vs. older, stabilized C that has been part of the subsoil SOC, which is now surfacing due to erosional soil losses on cropped hillslopes. Milled samples were acidified for 72 h with 12 M HCl vapor bath in a class desiccator and neutralized over NaOH pellets at 65 °C (Komada et al., 2008). The samples were measured on a MIni
205   CArbon DAta System (MICADAS), using Accelerator Mass Spectroscopy (AMS) at the Laboratory of Ion Beam Physics at ETH Zurich, Switzerland (Ruff et al., 2007). For soil reference profiles in forests, composites were created out of three field replicates per topographic position and measured in 0–10,cm, 30–40,cm, and 60–70,cm and measured on a MICADAS at the Max Planck Institute for Biogeochemistry (Jena, Germany). Radiocarbon activities are reported as Fraction modern (*Fm*), representing the deviations of the ^{14}C/^{12}C ratio from 95 % modern oxalic acid standard (Stuiver and Polach, 1977).

210   #### 2.4.3 Plant available phosphorus

Plant available P was measured on sieved forest and all hillslope soil samples by using the resin extraction method. This method is based on the first part of the Hedley extraction protocol (Hedley et al., 1982): 5.3 cm^2 anion exchange membranes (resins; VWR International, Material number 551642S) were used per g^{-1} dry soil and activated with 0.5 M NaHCO$_3$ (pH 8.5). Milli-Q water was added to the soil and the membranes were used to sorb P from the solution by horizontally shaking
215   for 16 h. The resin extraction was stopped and P was released from the membranes in 0.5 M H$_2$SO$_4$ for 1.5 h on a horizontal shaker (1.25 mL cm^{-2} membrane). All extractions were performed at effective soil pH. Phosphate in the H$_2$SO$_4$ solution

was colorimetrically quantified on a microplate photometer (Tecan Infinite M200, Tecan Austria GmbH, Austria) using the malachite green method (D'Angelo et al., 2001).

2.5 Estimation of soil and carbon loss on eroding hillslopes

220 Loss rates of soil and carbon on cleared hillslopes were estimated by comparing hillslope topsoil SOC contents to undisturbed old-growth forest profiles. This approach assumes that depth profiles of SOC contents in the original, pre-erosion hillslope profiles resembled the depth profiles of undisturbed forest profiles. Although forest reference profiles (hillslopes and plateaus) did not show any indication of erosion (results not shown; see Doetterl et al. (2021a)), such calculations likely overestimate erosion rate calculations solely based on SOC comparisons. Despite the comparability of the rates to other literature, such

225 results need to be interpreted carefully. We therefore interpret SOC losses compared to forest reference profiles as the combined effect of SOC losses due to land conversion and its effect on (i) lower plant C inputs, (ii) increasing microbial C turnover and (iii) increasing C losses due to higher erosion rates under cropland. The procedure was as follows: Firstly, the SOC content of all forest replicates was averaged for each depth increment (0–1 m depth with 10 cm increments, $n = 9$; Doetterl et al. (2021a, b)). Then, for all eroding hillslopes (cropland, abandoned, *Eucalyptus* sites), the equivalent depth in the undisturbed forest profile

230 was determined by matching hillslope topsoil SOC contents to the given SOC content in the averaged forest profile. Thus it was assumed that the hillslope had eroded and lost the same amount of SOC as was present above the calculated depth in the forest profiles. A soil loss rate ($cm\,yr^{-1}$) was calculated by dividing the matched depth by the time since deforestation. The volume of lost SOC (in $t\,ha^{-1}$) was estimated by summing the SOC stocks above the previously calculated depth in the forest profile. These estimations were only possible in the mafic region due to the lack of an observed effect of time since deforestation on

235 SOC content in the felsic region.

2.6 Data handling and statistical analyses

All statistical analyses and graphical visualizations were performed using the R language (R Core Team, 2023) and RStudio (Posit team, 2023). For importing the BRUKER binary files, we used the R package `opusreader2` version 0.6.2.9000 (Baumann et al., 2024), the package `prospectr` version 0.2.7 (Stevens and Ramirez-Lopez, 2024) for infrared data resampling

240 and pre-processing, and the package `resemble` version 2.2.3 for chemometrics and calibration modeling (memory-based learning; Ramirez-Lopez et al. (2024)). For mapping, we used the R packages `ggplot2` version 3.5.1 (Wickham, 2016), `terra` version 1.7-74 (Hijmans, 2024) and `geodata` version 0.5-9 (Hijmans et al., 2024), the latter providing spatial data such as country borders, elevation and land cover raster. For testing the statistical significance of SOC, TN, P_{resin}, and ECEC differences between the land use and years since deforestation, Type III ANOVA was performed (unbalanced data) on the

245 log-transformed SOC, TN, ECEC and P_{resin} data (to fulfill the model assumptions). A pairwise comparison was done using the Tukey-HSD test. The relative changes of SOC, TN, ECEC, and P_{resin} on the hillslopes were calculated compared to the forest means using (hillslope SOC content - mean forest SOC content) / mean forest SOC content x 100). Uncertainties were calculated using standard error of the means (standard error of the means / mean forest SOC content x 100).

3 Results

3.1 Change of SOC with time after deforestation

In the mafic region, a significant decrease of topsoil SOC content with time after deforestation was observed (Figure 2). Average SOC content on mafic parent material ranged from $64.4\,\mathrm{g\,C\,kg^{-1}}$ under forest decreasing to $23.3\,\mathrm{g\,C\,kg^{-1}}$ under cropland cleared >60 years ago. Abandoned fields had an average SOC content of $19.7\,\mathrm{g\,C\,kg^{-1}}$, while soil under *Eucalyptus*, cleared 40–60 years and >60 years ago, had an average of $40.5\,\mathrm{g\,C\,kg^{-1}}$ and $38.1\,\mathrm{g\,C\,kg^{-1}}$, respectively. Mean relative change (+- standard error of the means) in topsoil SOC content compared to the forest mean were -64 % (+- 9 %) on cropland cleared >60 years ago, -69 % (+- 15 %) on abandoned sites, and -41 % (+- 12 %) in soil under *Eucalyptus* monoculture cleared >60 years ago (Figure D3).

In topsoils of the felsic region, SOC did not exhibit a decrease along the deforestation chronosequence as in the mafic region. Nevertheless, SOC content in degraded cropland was similar to its equivalent in the mafic region. Forest topsoils in the felsic region (mean of $36.5\,\mathrm{g\,C\,kg^{-1}}$) did not show significantly higher SOC content than nearby croplands (mean of $30.9\,\mathrm{g\,C\,kg^{-1}}$), even though a slight, but not significant trend towards lower SOC content with time since deforestation was visible. Soils under *Eucalyptus* had the highest mean SOC content ($59.6\,\mathrm{g\,C\,kg^{-1}}$) when sites were cleared 2–7 years ago and the lowest content ($20.6\,\mathrm{g\,C\,kg^{-1}}$) when cleared >60 years ago (Figure 2).

3.2 Fraction modern in topsoil

In the mafic region, *Fm* ranged between 1.03–1.05 in the topsoils of the depth-explicit forest reference profiles and decreased to 0.72–0.78 at 60–70 cm soil depth. In forest reference profiles within the felsic region, *Fm* ranged between 1.04–1.07 in topsoil (0–10 cm) and decreased to 0.46–0.77 at 60–70 cm soil depth. Cropland topsoils in the mafic region cleared >60 years ago had lower *Fm* values (mean of 0.81 in 0–10 cm) than the corresponding forest reference topsoils (mean of 1.05; Figure 3a). These measured topsoil cropland *Fm* values corresponded to the depths of 30–40 cm and 60–70 cm in the reference forest profiles (*Fm* = 0.68–0.85; Figure 3a). In contrast, topsoils of cropland in the felsic region cleared >60 years ago had comparable *Fm* values to sites in the forest reference profiles (average of 1.01 in 0–10 cm).

3.3 Soil erosion rates and lifetime of cropped hillslopes in the mafic region

The current SOC content in cropland, abandoned, and *Eucalyptus* monocultures topsoils cleared >60 years ago was equivalent to the average SOC content of the forest soil at depths of 48, 62, and 25 cm soil depths, respectively (Figure 4). The resulting losses of SOC stocks (sum of average forest SOC stocks above the calculated depths) are estimated to be $131\text{–}290\,\mathrm{t\,C\,ha^{-1}}$ (Figure 4). We estimated that the soil above the depth of 22.5 cm had been lost from the hillslope over the last 40–60 years indicating an average loss rate of $0.5\,\mathrm{cm\,yr^{-1}}$. Based on this loss rate, we calculated conversion ages of 86–130 years for cropland sites and 111–168 years for abandoned sites (for the sites with >60 years since deforestation).
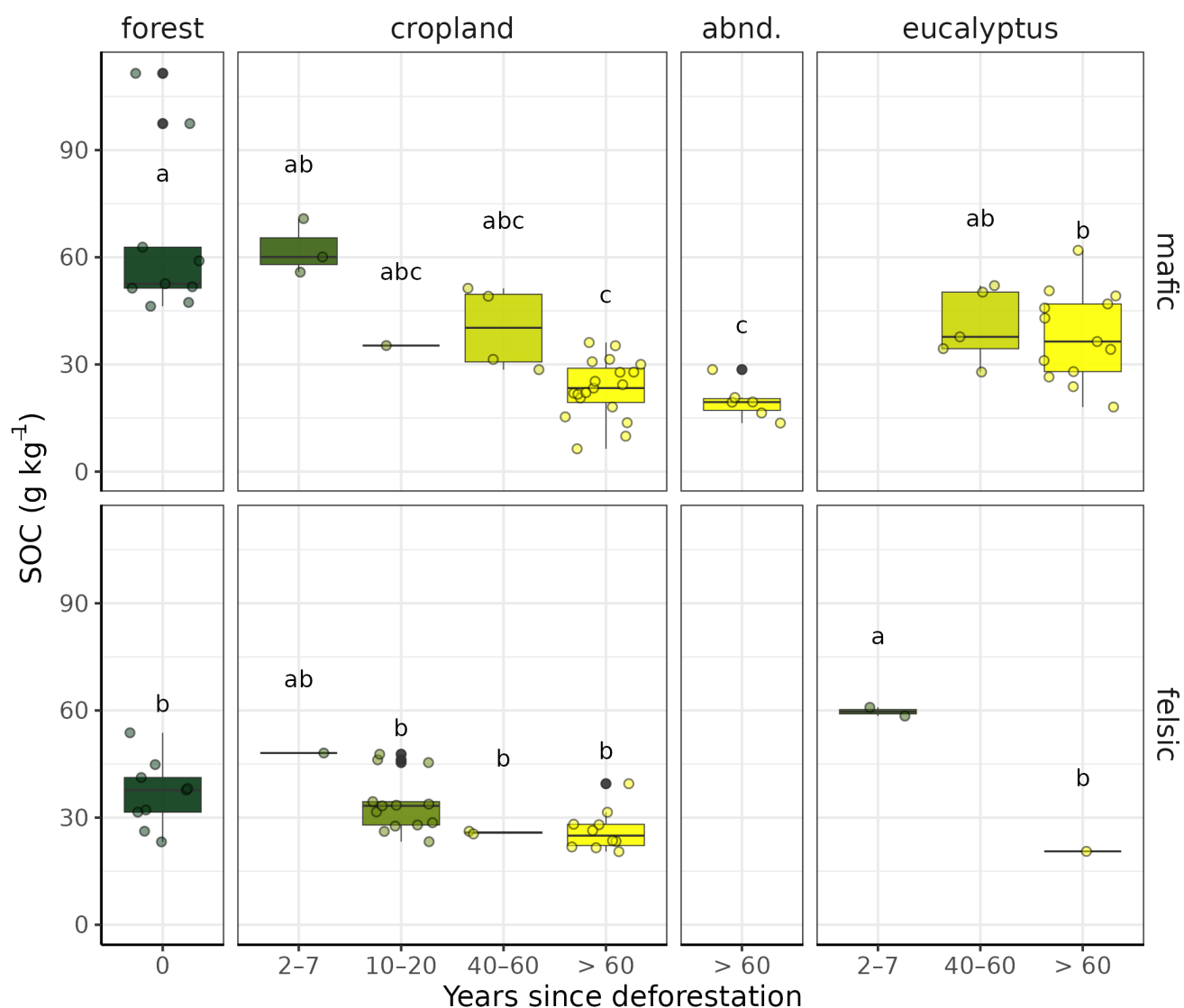
Figure 2. Soil organic carbon (SOC) in 0–10 cm in soils developed on mafic (top) and felsic (bottom) parent material. Green to yellow colors correspond to the deforestation chronosequence (0, 2–7, 10–20, 40–60, >60 years after deforestation). Data are split by land cover into forest, cropland, abandoned (abnd.), and *Eucalyptus*. Within each geology (mafic and felsic), letters indicate significant differences between the sites (ANOVA of log transformed SOC with a subsequent Tukey Post-Hoc test, significance level 0.05).
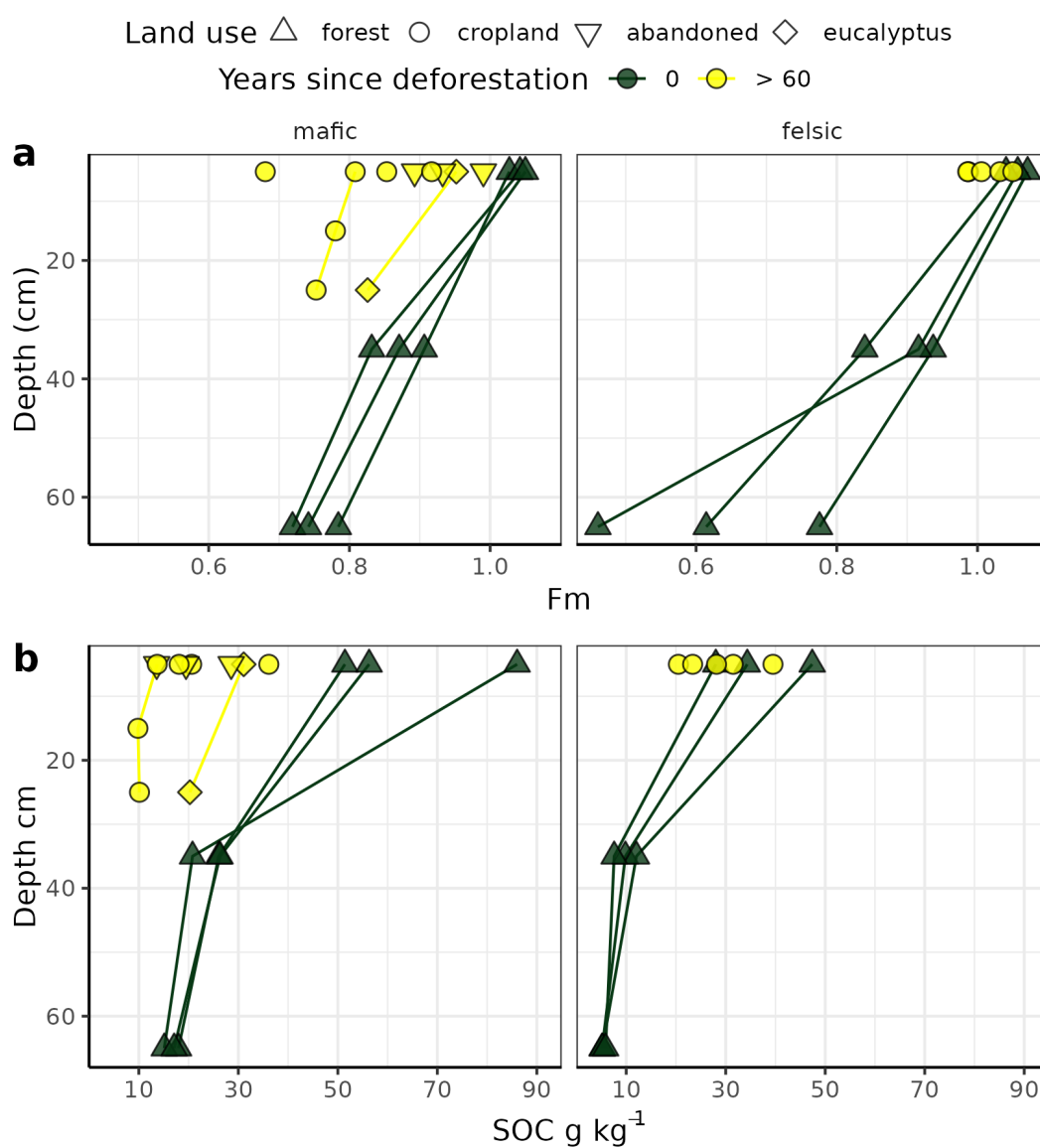
Figure 3. a: Fraction modern (*Fm*), and **b**: soil organic carbon (SOC) versus soil depth in degraded hillslopes of cropland (circles), *Eucalyptus* (diamonds), abandoned cropland (upside down triangles) sites cleared >60 years ago (yellow symbols). Forest reference profiles from Doetterl et al. (2021a, b) are plotted as green triangles.
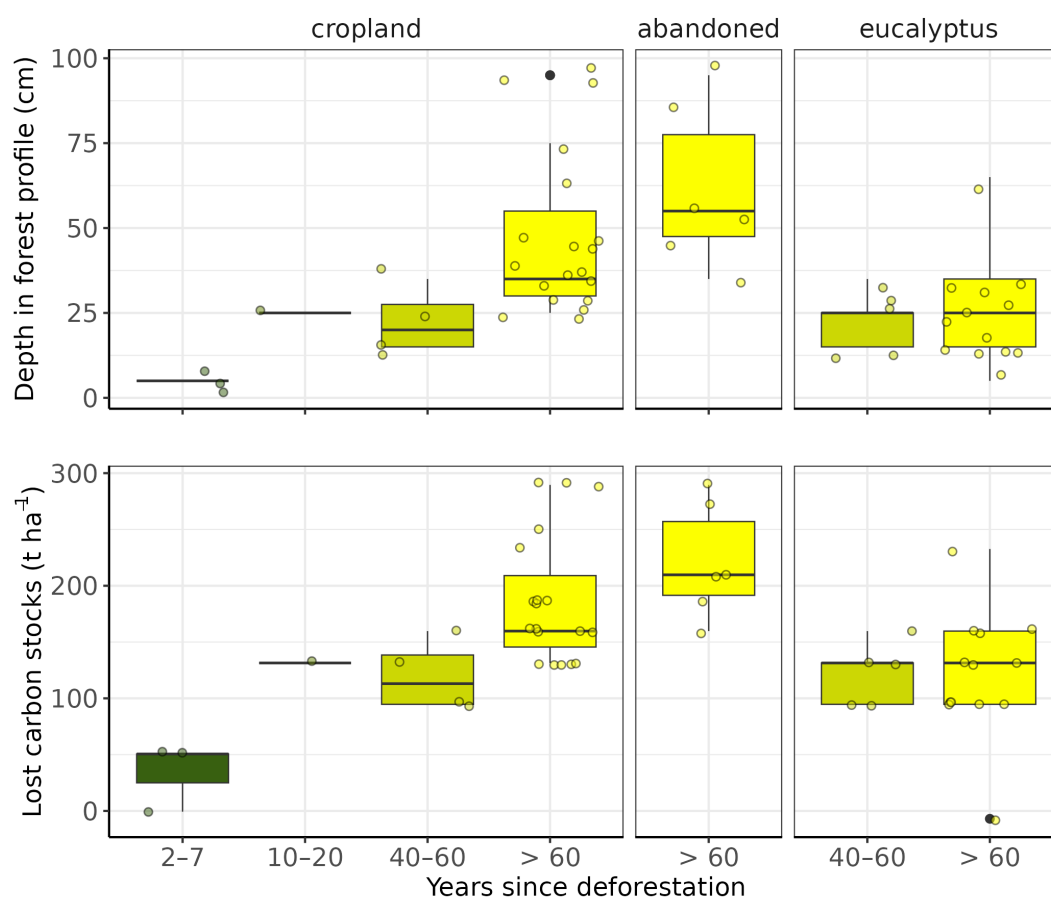
Figure 4. Depth in forest profiles based on mean soil organic carbon (SOC) content that correspond to the SOC contents of hillslope topsoils in 0–10 cm in the mafic region (top), and lost carbon stocks (sum of the mean carbon stocks of the forest profiles layers above each corresponding calculated depth). Green to yellow colors show the deforestation chronosequence (0, 2–7, 10–20, 40–60, >60 years after deforestation). Data are split by land cover into forest, cropland, abandoned, and *Eucalyptus*. Note that the estimated depth in forest profile and lost carbon stocks were only generated for the mafic region since there was no statistically significant decline in SOC along the chronosequence in the felsic region.

3.4 Changes to soil fertility proxies after deforestation

3.4.1 Total nitrogen

TN followed a similar pattern as SOC in both parent materials. In mafic soils, a strong decrease of TN content was observed from forest sites (mean TN of $6.0\,\mathrm{g\,N\,kg^{-1}}$) to soils under cropland with age since cropland conversion (2–7 years: $3.5\,\mathrm{g\,N\,kg^{-1}}$, 10–20 years: $2.5\,\mathrm{g\,N\,kg^{-1}}$, 40–60: $3.2\,\mathrm{g\,N\,kg^{-1}}$, >60 years: $1.9\,\mathrm{g\,N\,kg^{-1}}$), while abandoned sites had the lowest mean TN levels ($1.7\,\mathrm{g\,N\,kg^{-1}}$). Soils under *Eucalyptus* had an average TN content of 3.0 and $2.5\,\mathrm{g\,N\,kg^{-1}}$, cleared 40–60 and >60 years ago, respectively (Figure 5). The average relative changes compared to the forest for cropland and abandoned cleared >60 years ago ranged from -68 % (+- 6 %) to -72 % (+- 9 %) (Figure D3). In the felsic region, topsoil TN exhibited stronger decreases than SOC with time since deforestation and conversion to cropland; the average TN content in forests was $3.7\,\mathrm{g\,N\,kg^{-1}}$ and decreased to $2.4\,\mathrm{g\,N\,kg^{-1}}$ under cropland cleared >60 years ago (Figure 5). In soils under *Eucalyptus*, TN content was 4.5 and $1.4\,\mathrm{g\,N\,kg^{-1}}$ for sites cleared 2–7 and >60 years ago, respectively (Figure 5). The average relative TN change on cropland sites cleared >60 years ago was -36 % (+- 9 %) (Figure D3).

3.4.2 Effective cation exchange capacity

In topsoils of the mafic region, ECEC ranged from a minimum of $1.7\,\mathrm{cmol_c\,kg^{-1}}$ under *Eucalyptus* on sites cleared >60 years ago to $20.6\,\mathrm{cmol_c\,kg^{-1}}$ under forest at an overall average of $7.6\,\mathrm{cmol_c\,kg^{-1}}$ regardless of land use and time since deforestation. Mean relative changes of ECEC in soils under *Eucalyptus* monocultures were -55 % (+- 13 %) and -61 % (+- 20 %) on sites 40–60 and >60 years after deforestation. In the felsic region, topsoil ECEC ranged from 7.4 to $24.4\,\mathrm{cmol_c\,kg^{-1}}$, with an overall mean of $13.2\,\mathrm{cmol_c\,kg^{-1}}$. Lowest values were observed in cropland topsoils cleared 10–20, 40–60, and >60 years ago. Highest ECEC values were observed in forest topsoils (Figure 5).

3.4.3 Plant available phosphorus

In the mafic region, plant available P content (P_{resin}) decreased along the deforestation chronosequence. P_{resin} was highest in forest soils ($6.7\,\mathrm{mg\,kg^{-1}}$) and lowest in abandoned hillslope soils cleared >60 years ago ($0.6\,\mathrm{mg\,kg^{-1}}$). Croplands that were cleared >60 years ago had a mean value of $2.9\,\mathrm{mg\,kg^{-1}}$ and *Eucalyptus* topsoils had mean values of 1.4 and $1.2\,\mathrm{mg\,kg^{-1}}$ when cleared 40–60 and >60 years ago, respectively (Figure 5). Compared to the forest, mean relative changes in P_{resin} were between -82 % (+- 18 %) in *Eucalyptus* topsoils >60 years since deforestation and -92 % (+- 25 %) for abandoned croplands (Figure D3). In the felsic region, however, P_{resin} content did not decrease along the deforestation chronosequence and under the different land uses. Mean values ranged from $11.5\,\mathrm{mg\,kg^{-1}}$ in forest topsoils, 1.7–$7.0\,\mathrm{mg\,kg^{-1}}$ in cropland topsoils, and 6.0 under *Eucalyptus* on sites with 2–7 years since deforestation (Figure 5).
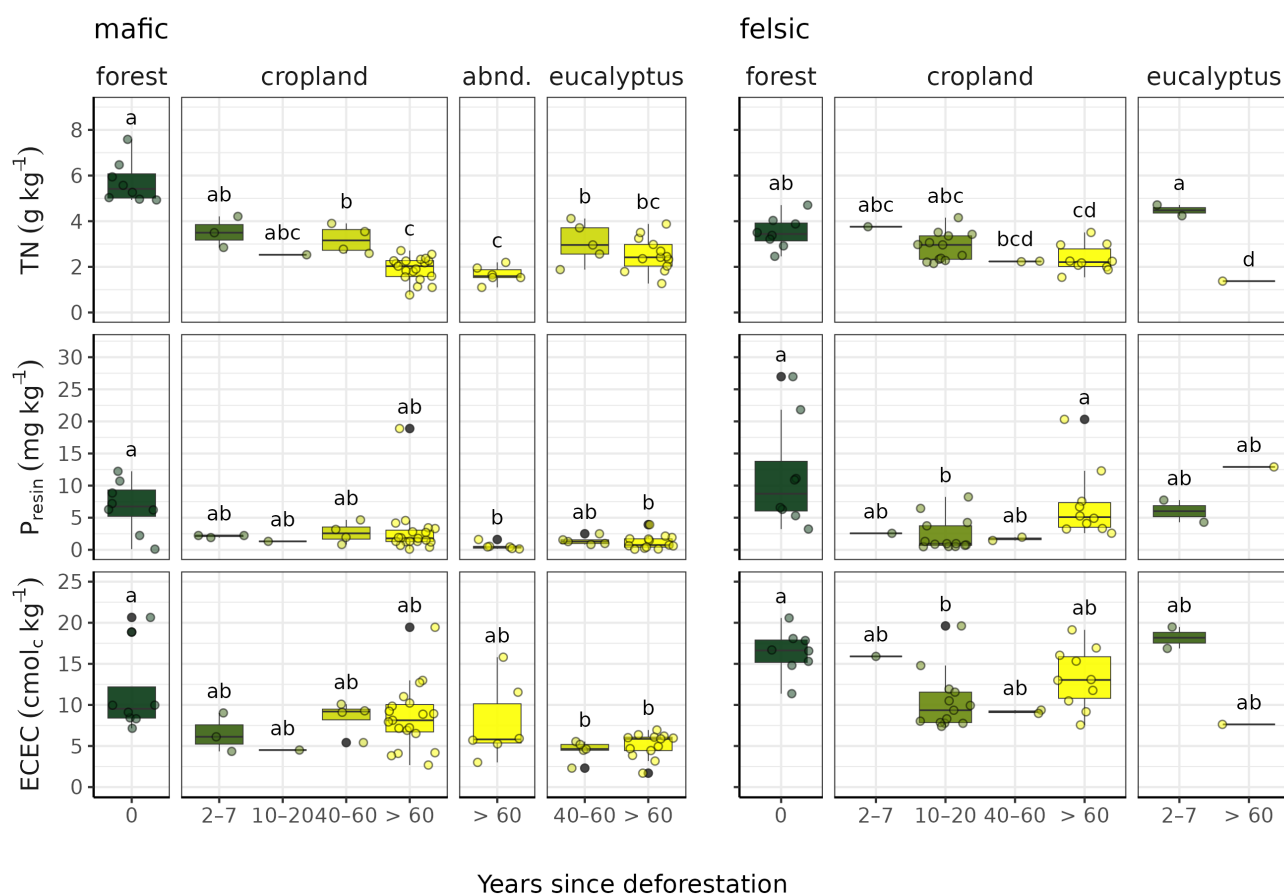
Figure 5. Total nitrogen (TN), plant available P (P$_{resin}$), and effective cation exchange capacity (ECEC) in 0–10 cm under forests, croplands, *Eucalyptus*, and on abandoned sites (abnd.) along the deforestation chronosequence (0, 2–7, 10–20, 40–60, >60 years since deforestation) in soils developed on mafic (left) and felsic (right) parent material. Different letters indicate significant differences to the other groups of the same geology (ANOVA of log transformed response variables with a subsequent Tukey Post-Hoc test, significance level 0.05).

3.5 Land abandonment and relation to solution chemistry and fertility

In the mafic region, numerous hillslopes were found to be abandoned due to infertility. This was not the case, however, in the felsic region, where only one highly degraded hillslope under *Eucalyptus* (cleared >60 years ago) could be sampled. Mean pH_{CaCl_2} values (mafic: 4.17, felsic: 5.24; Figure 6b, Figure 6f), and the sum of base cations (mafic: $5.21\,cmol_c\,kg^{-1}$, felsic: $12.90\,cmol_c\,kg^{-1}$; Figure 6c, Figure 6g) were lower in the mafic compared to the felsic region. Consequently, mean Al^{3+} values were generally higher in topsoils of the mafic than of the felsic region (mafic: $2.4\,cmol_c\,kg^{-1}$, felsic: $0.4\,cmol_c\,kg^{-1}$; Figure 6a, Figure 6e). In the mafic region, decreasing pH_{CaCl_2} significantly co-varied with decreasing sum of base cations (Figure 6d) and increasing Al^{3+} (Figure 6b). As the ECEC decreased, Al^{3+} increased (Figure 6a). Sites with low pH_{CaCl_2} values, high Al^{3+}, and low base cations were dominated by *Eucalyptus* monocultures, abandoned cropland sites, and forests (Figure 6a, Figure 6b). For soils in the felsic region, pH_{CaCl_2} values significantly and positively correlated with the sum of base cations (Figure 6g). In contrast, there was no clear relationship between exchangeable Al^{3+} and either pH_{CaCl_2} or ECEC (Figure 6e, Figure 6f). Topsoils under *Eucalyptus* monoculture, where conversion after deforestation happened just 2–7 years ago, had the highest Al^{3+} values in the felsic region (which were still much lower than for most soils in the mafic region; Figure 6e, Figure 6f).

3.6 Correlations of ECEC, clay, and reactive metals with SOC content

ECEC was positively correlated with SOC in soils of the felsic region (R^2 = 0.28, p < 0.01) but not in the mafic region (no significant correlation; Figure 7), where ECEC values were extremely low ($<10\,cmol_c\,kg^{-1}$). Instead, there was a strong correlation of SOC with reactive Al and Fe (Al_{PyOx} and Fe_{PyOx}) in soils of the mafic region (Al_{PyOx}: R^2 = 0.54 and p < 0.01, Fe_{PyOx}: R^2 = 0.36 and p < 0.01; Figure 7) but not of the felsic region. Differences between the two geochemical regions were also observed for the content of these two reactive metal phases, with Al_{PyOx} ranging between 0.0–0.6 % and Fe_{PyOx} ranging between 0.0–2.1 % in soils of the felsic region and Al_{PyOx} ranging between 0.0–1.2 % and Fe_{PyOx} ranging between 0.0–2.7 % for soils of the mafic region. Similarly, we observed a decrease of reactive Al and Fe phases with time after deforestation for soils in the mafic region, while these differences were not observed for soils of the felsic region. Although clay content ranged from 28–76 % and 29–59 % in soils of the mafic and felsic region, respectively, SOC did not correlate positively with clay content in either region. In fact, a slight but significant negative correlation of SOC and clay was observed in the mafic region (R^2 = 0.18, p < 0.01; Figure 7).

4 Discussion

4.1 Parent material and volcanic ash determine SOC loss after deforestation

A strong decrease of SOC content was observed along the deforestation chronosequence in the mafic region (Figure 2), which we attribute to post-deforestation erosion. It is widely accepted that deforestation causes severe losses of tropical SOC (e.g., Dechert et al., 2004; Wasige et al., 2014; van Straaten et al., 2015; Hombegowda et al., 2016; Namirembe et al., 2020). Particularly fast loss of SOC following forest conversion to cropland has been shown for a wide variety of tropical agroecosystems
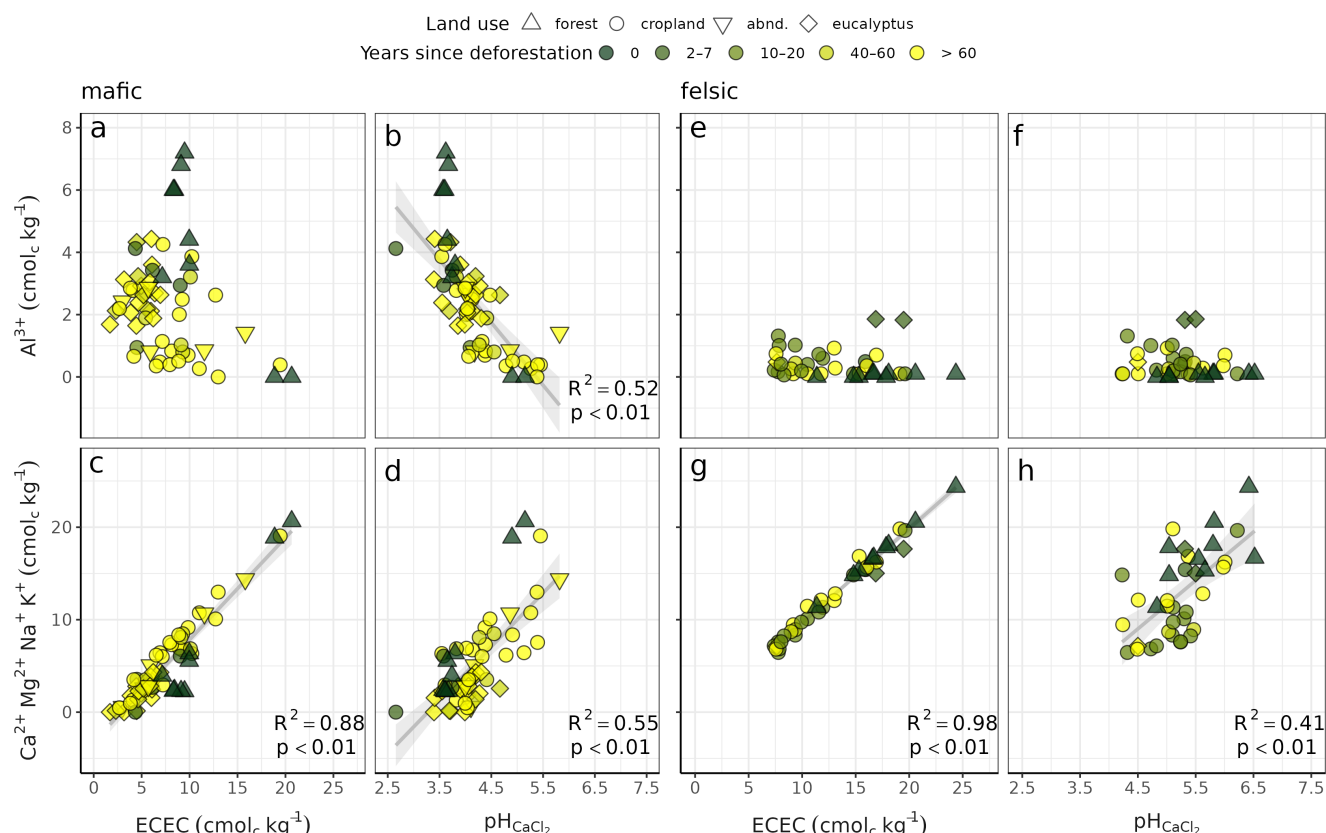
Figure 6. Correlation of effective cation exchange capacity (ECEC) and pH_{CaCl_2} vs. Al^{3+}, sum of base cations in topsoils 0–10 cm developed on mafic (left; a–d) and felsic parent material (right; e–h). Linear regression lines, R^2 and p-value are indicated where $p < 0.05$.

(Nye and Greenland, 1964; Detwiler, 1986; Davidson and Ackerman, 1993; Veldkamp et al., 2020). However, these studies
340 generally investigated geomorphologically more stable landforms (i.e. flat topography). Interestingly, our study in geomorpho-
logically active and quickly eroding landscapes also shows that most SOC loss occurs within the first years after conversion
(Figure 2, Figure 4, Figure D3), contradicting our first hypothesis where we expected more continuous losses of SOC over time
after deforestation. Due to high erosion rates in the sloping landscapes of the study region, the relative change of SOC content
is higher compared to stable landforms, particularly for the mafic region (up to -69 %, Figure D3).

345

In the felsic region, soil fertility and volcanic activity influenced SOC content more than land cover. No clear effect of
deforestation on SOC was observed: forest soils were found to have lower SOC content than the cropland sites converted 2–7
years ago (Figure 2, Figure D3), likely indicating a difference in soil chemical and physical properties between the two land
covers in the felsic region (Doetterl et al., 2021a, b). Based on local observations, we assume that croplands in the felsic region
350 were established on more fertile soils, while forests were selectively left intact on less fertile soils. Moreover, soils in the felsic
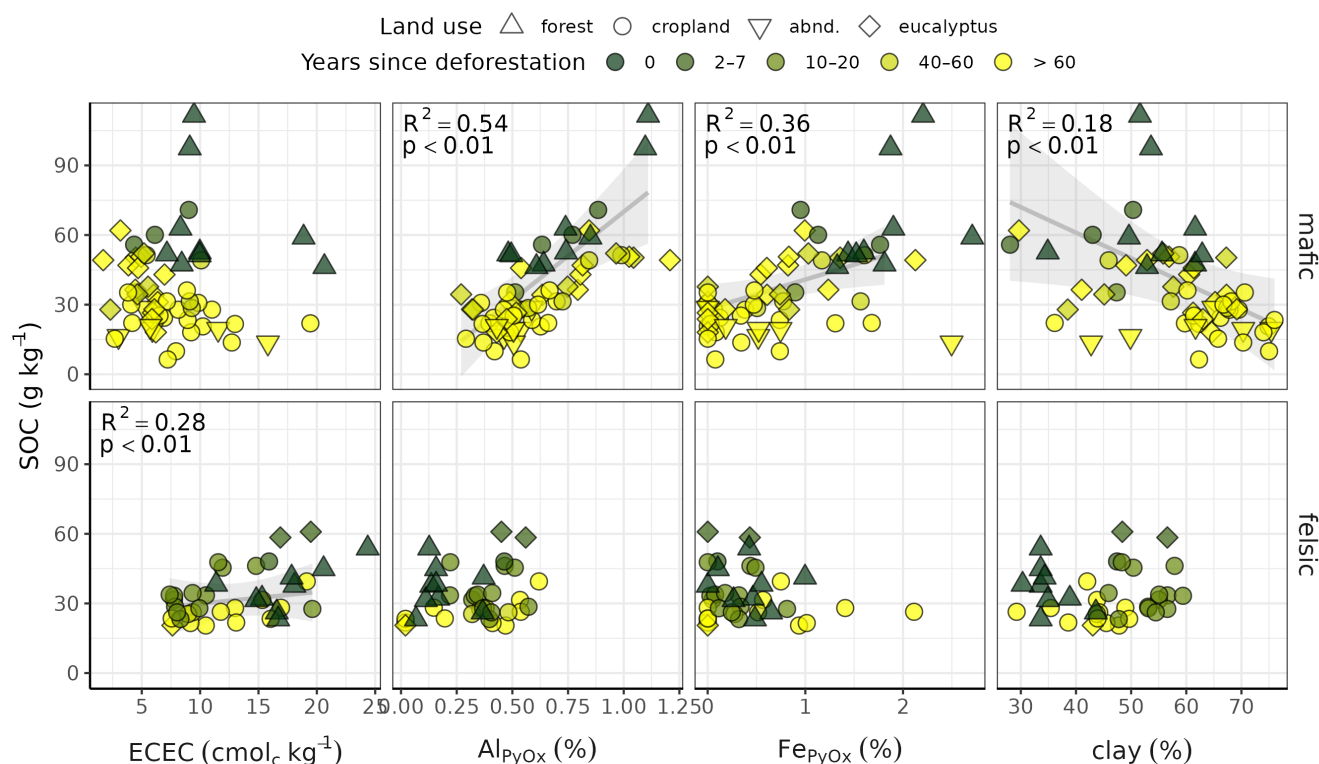
Figure 7. Soil organic carbon (SOC) vs. ECEC, pyrophosphate and oxalate extractable aluminum (Al_{PyOx}) and iron (Fe_{PyOx}), as well as clay content along the chronosequence of deforestation in topsoils (0–10 cm) developed on mafic and felsic parent material. Linear regression lines, R^2, and p-values are indicated where p < 0.05.

region were unevenly affected by mineral replenishment from mid-Holocene volcanism, likely driving some of the observed geochemical differences between the included forest sites in the region. This interpretation is supported by prior observations showing less influence of allophanes and therefore volcanic ashes in forest soils compared to cropland sites (Al_p:Al_o ratio = 0.9; Figure D7) (Nanzyo et al., 1993) in this region. These findings suggest that soils with high fertility due to volcanic inputs

355 can sustain longer and more productive farming and thus impede land abandonment.

4.2 Metals, and not clay, are the key drivers of SOC contents

Our results highlight the distinct C stabilization mechanisms on weathered soils of the humid tropics, which are an understudied region (Van Oost and Six, 2023). In contrast to many regions of the world (Angst et al., 2018; Quesada et al., 2020; Soares and Alleoni, 2008; Souza et al., 2017) clay and SOC content were not significantly correlated in either of the two geochemical

360 regions (Figure 7). The lack of this relationship may be caused by the fact that old and deeply weathered soils of the humid tropics are dominated by clay-sized minerals with low reactive surface areas. Such clays form fewer organo-mineral associa-

tions and aggregates (Six et al., 2002), which could provide protection against microbial predation of SOC (Kögel-Knabner et al., 2008). Negative or missing relationships between SOC contents and clay have also been observed in other parts of the tropics (Araujo et al., 2017; Bruun et al., 2010; Dick et al., 2005; Heri-Kazi and Bielders, 2021). Despite these results, clay is 365 still often used as a universal predictor for SOC in many large-scale studies. This assumption undoubtedly leads to erroneous assumptions regarding the SOC stabilization potential of tropical soils (e.g., Coleman and Jenkinson, 1996; Wieder et al., 2015; Bukombe et al., 2022; Reichenbach et al., 2023).

Particularly in the mafic region, our study emphasizes the importance of reactive metal phases in understanding SOC turnover 370 and stability, as also highlighted by Wu et al. (2023) and Rasmussen et al. (2018) (Figure 7). Sesquioxides can form resistant (e.g., Doetterl et al., 2015; Hall and Thompson, 2022; Kirsten et al., 2021) and old (Jagadamma et al., 2010; Mikutta and Kaiser, 2011; Stoner et al., 2023; Tisdall and Oades, 1982) mineral-associated organic matter. The limited C sorption suggests that fresh C is minimally stabilized via new surfacing minerals (concept of the geomorphic pump; Stallard (1998)). Several meters of weathered subsoil need to erode before less weathered minerals appear closer to the surface. However, our obser-375 vations indicate that the thick subsoil layers have not fully been eroded (e.g. depths of 5–8 m, Figure D6, Figure D8), and thus the weathering front has not yet reached the more nutrient-rich parent material. On one hand, fresh plant input to soil is scarce (mainly roots and root exudates) since most of the above-ground crop material in tropical African subsistence farms is harvested (Duncan et al., 2016; Giller et al., 2009). On the other hand, fresh plant input that does end up being incorporated into the soil might be rather labile and decompose quickly. However, this is important as the apparent C saturation due to com-380 paratively unreactive sesquioxides, combined with the strong (metal-related) stabilization of old SOC, likely explains the low SOC content of cropland and abandoned sites in the mafic region, which were cleared >60 years ago ($\sim$19 g kg^{-1}, Figure 2).

In the felsic region, the lack of reactive Al and Fe seemed to limit SOC stabilization, as we did not observe correlations between reactive metals and SOC (Figure 7). In this geochemical region reactive Al and Fe content that can support organo-385 mineral complexation over long timescales (Kallenbach et al., 2016; Kögel-Knabner et al., 2008; Lavallee et al., 2020) were substantially lower than in the mafic region. Comparatively young SOC ages in croplands of the felsic region (Figure 3) and the connection to key fertility indicators such as ECEC (Figure 7) highlight the importance of fresh C inputs to avoid degradation and the subsequent decrease in crop yields. This suggests that with a higher soil fertility and crop productivity than in the mafic region, more fresh C enters the SOC pool, despite a comparatively lower SOC stabilization potential. This interpretation 390 is supported by findings in other tropical regions that show the residence time of organic C in soils is short when reactive minerals to stabilize C are lacking (Paul et al., 2008; Reichenbach et al., 2023). More research is needed to better understand SOC stabilization mechanisms in the felsic region, for example by exploring how the region's internal presence or absence of volcanic ashes (determined via x-ray fluorescence) or soil pH might impact SOC (Veldkamp et al., 2020). Our second hypothesis (greater SOC stabilization in the mafic region due to higher contents of clay and reactive metals) can be rejected. 395 Instead, the higher fertility levels in the felsic region likely lead to increased fresh organic matter input, resulting in higher SOC content. In contrast, the reactive surfaces in the mafic region are limited.

4.3 Estimated erosion rates and the lifetime of cropped hillslopes in the mafic region

The estimated erosion rates, based on SOC comparisons between hillslope topsoils and forest profiles, and their alignment with other studies, indicate minimal replacement of eroded SOC in cropland, *Eucalyptus*, and abandoned hillslope topsoils. The cal-
400 culated erosion rate of $0.5\,\mathrm{cm\,yr^{-1}}$ corresponds well with previous measurements of erosion rates of 0.3–$0.7\,\mathrm{cm\,season^{-1}}$ (sum of reported rill and gully erosion; approx.: 0.6–$1.1\,\mathrm{cm\,yr^{-1}}$) on croplands in South Kivu by Heri-Kazi and Bielders (2021). Using $^{239+240}$Pu fallout radionuclides, Wilken et al. (2021) estimated similar erosion rates of $0.4\,\mathrm{cm\,yr^{-1}}$ in two catchments in South Kivu ($51.4\,\mathrm{t\,ha^{-1}\,yr^{-1}}$; assuming a bulk density of $1.25\,\mathrm{g\,cm^{-3}}$). Modeled erosion rates and estimates using remote sensing for the region were within the same range but more variable ($30\,\mathrm{t\,ha^{-1}\,yr^{-1}}$ (Karamage et al., 2016), $138\,\mathrm{t\,ha^{-1}\,yr^{-1}}$
405 (Kulimushi et al., 2021)). As a consequence of the agreement between these non-carbon-based erosion estimates with our SOC observations and the old SOC signatures (Figure 3), we conclude that little replacement of eroded C takes place on the cropped hillslopes.

The erosion rates and conversion ages reveal rapid degradation and abandonment of croplands on hillslopes, thereby under-
410 scoring the urgent need for sustainable farming. Interestingly, Drake et al. (2019) estimated that soil from an average depth of $0.5\,\mathrm{m}$ was eroded and mobilized into the rivers in fully deforested catchments in the same region, which would indicate a conversion age of approximately 100 years (given our average erosion rate of $0.5\,\mathrm{cm\,yr^{-1}}$). Overall, these estimated conversion ages correspond well with the reported history of the region, which was characterized by scattered settlements and kingdoms until the end of the 19th century and intensified deforestation with colonization in the beginning of 1900 (Melkebeke, 2020;
415 Newbury, 2010). Ultimately, if hillslopes are abandoned after approximately 100–170 years, as our data indicate, then the region will face extreme challenges in the near future. A large proportion of the hillslopes around Bukavu were cleared in the early 20th century. These hillslopes thus already exceed the 100 years lifespan, leaving only a few decades left for farming if no measures are taken to preserve soil fertility and introduce more sustainable and conservation farming approaches. Unfortunately, these timespans are probably conservative, because population densities in the region rapidly increase (WorldPop,
420 2020). Furthermore, in the three territories of our study area (Walungu, Kabare and Kalehe), about $70\,\%$ of the agricultural land has inclinations of $>10\,^\circ$ (own analyses, Figure D9; sources: SRTM $30\,\mathrm{m}$ and ESA-CCI S2 prototype Land Cover $20\,\mathrm{m}$ map of Africa 2016).

4.4 Land abandonment is driven by nutrient limitations and Al toxicity

Low fertility, high soil acidity, and Al toxicity likely cause land abandonment of croplands in the mafic region. The low values
425 of key fertility indicators in abandoned hillslope topsoils of the mafic region (ECEC, TN, and bioavailable-P / $\mathrm{P_{resin}}$, Figure 5) indicate that sustainable management needs to address a multitude of elements to avoid land abandonment. Also, imbalanced nutrient stoichiometries such as low $\mathrm{P_{resin}}$:TN ratios (Figure D5) might negatively influence plant growth and microbial functions causing further unfavorable conditions for biological processes (Bauters et al., 2022; Bertrand et al., 2019). Moreover, low Ca:Al ratios are unfavorable for plants (Hedin et al., 2003), which is likely the case in soils of the mafic region in our

10.5194/egusphere-2025-4625
2025-10-05
Author(s) 2025. CC BY 4.0 License

study. In parallel, our data suggests that land abandonment may be driven by increasing soil acidity and Al toxicity, even if other fertility indicators such as SOC and TN remain favorable. As pH decreases towards values <4, a large proportion of Al is mobilized into soil solution as Al^{3+} (Sparks et al., 2022), where it can be taken up and cause toxic conditions for crops (Sanchez and Logan, 1992). From informal conversations with farmers and our later soil data analyses, we learned that slopes with such low pH and high Al^{3+} were not used for cropping anymore due to the low performance of crops, and instead abandoned or used for *Eucalyptus* monocultures.

Geochemical soil properties in both regions (Figure 5, Figure 6, Figure D7) indicate that volcanic inputs slowed soil degradation in the felsic region, highlighting the role of geochemical differences in maintaining soil fertility. Mid-Holocene carbonate volcanism appears to prevent land abandonment due to the maintenance of acceptable pH values and soil fertility levels (Bailey et al., 2005; Barker and Nixon, 1989). This supports our third hypothesis that differences in the timescale of land abandonment are to be expected due to geochemically contrasting fertility conditions in soils derived from different parent material and varying levels of volcanic ashes. However, erosion rates in the felsic region were modeled to be in a similar range as for the soils in the mafic region (Karamage et al., 2017; Kulimushi et al., 2021). Furthermore, Wambede et al. (2016) showed in field trials soil losses of up to $25\,\mathrm{t\,ha^{-1}}$ for one cropping season, which would equate to similar magnitudes as measured in our mafic sites (at least twice the amount). This indicates that under current agricultural practices, land abandonment due to a complete loss of the fertile, volcanic-ash improved layers can be expected on steep slopes also in the felsic region in coming decades.

4.5 *Eucalyptus* monocultures cause nutrient depletion

In the mafic region, our data suggest that the planting of *Eucalyptus* can restore SOC content to a level of croplands cleared 40–60 years ago (Figure 2), therefore recuperating only a small portion of SOC losses in topsoil caused by the initial deforestation and erosion. A similar increase of SOC under *Eucalyptus* has also been shown by Marín-Spiotta and Sharma (2013), Zhang et al. (2012), and Don et al. (2011), however, others have observed no effect or even a decrease of SOC in *Eucalyptus* plantations (Cook et al., 2016; Fialho and Zinn, 2014; Harper et al., 2012; Lima et al., 2006). Our results support this variation in effect since recovered SOC content under *Eucalyptus* monocultures was highly variable. Thus, our fourth hypothesis (*Eucalyptus* monocultures improving SOC stocks) was partially confirmed, however not to the degree of full SOC recovery. For the felsic region, we could not investigate the effect of *Eucalyptus* due to the small sample size.

While *Eucalyptus* plantations can thrive on degraded soils, our results suggest that they may also reduce soil fertility by lowering pH and increasing Al^{3+} toxicity. The tolerance of *Eucalyptus* to heavily degraded soils has been reported for many tropical systems (e.g., Bouillet et al., 2013; Korchagin et al., 2019; Laclau et al., 2003; Lemenih et al., 2004; Lima et al., 2006). Subsistence farmers in South Kivu often plant *Eucalyptus* on hillslopes to generate viable income via charcoal or timber production once crops no longer provide reasonable yields on degraded land (Brancalion et al., 2020). However, the monoculture plantations of these non-native trees can have strong negative effects on soil fertility proxies. First, in the mafic region, soil pH_{CaCl_2} drastically decreased under *Eucalyptus* and thus reduced ECEC to very low levels (Figure 5). Due to the fact that

Eucalyptus topsoil pH_{CaCl_2} and ECEC were lower than even those of abandoned hillslopes (Figure 1, Figure 5), we argue that
465   *Eucalyptus* plantations caused the additional acidification. Indeed, such a lowering of pH and ECEC by *Eucalyptus* has been
shown before (Kangela Matazi et al., 2023; Laclau et al., 2003, 2005). Second, Al^{3+} saturation of the soil solution, which
was on average 53 % across the *Eucalyptus* plantations (exchangeable Al^{3+} relatively to the ECEC; results not shown), was
extremely high and toxic for most crops (Sanchez and Logan, 1992).

470   In the felsic region, negative effects of *Eucalyptus* on soil fertility have not been found (Majaliwa et al., 2010), but our
data suggest that soils under such plantations may eventually exhibit similar detrimental impacts as seen in the mafic region.
However, our sample size for *Eucalyptus* sites in the felsic region is small for clear interpretations. Moreover, the majority of
these sites were only recently cleared and likely installed on relatively fertile soil to support the local tea industry rather than as
an alternative post-cropping land use. It therefore might take more time for soils of the felsic region under *Eucalyptus* to exhibit
475   the same negative effects on pH and ECEC as in the mafic region. There is no evidence that suggests that plantations in the
felsic region will show different fertility endpoints than described for the mafic region and elsewhere (Fiantis et al., 2019). The
problem of soil degradation through *Eucalyptus* will further be exacerbated with planned expansions of *Eucalyptus* plantations
(Lejeune et al., 2013; Lee et al., 2024). The lack of knowledge about precise plantation installation and harvest frequency adds
limitations to our understanding of short and long-term effects of *Eucalyptus* plantations and urgently calls for more research.
480   We conclude that the negative effects of *Eucalyptus* on soil fertility relativize partial improvements of SOC stocks that we
observed which falsifies our fourth hypothesis (*Eucalyptus* monocultures improving soil fertility due to erosion control).

5   Conclusions

We observed a rapid decrease of SOC, nitrogen, and bioavailable phosphorus in the mafic region after deforestation. In mafic
soils, SOC content was strongly correlated to mineral C stabilization through reactive metal phases but showed little capacity
485   to stabilize new C inputs. In felsic soils, no clear effect on SOC content and soil fertility proxies was observed with increasing
time since deforestation. In this geochemical region, SOC content was tied to soil fertility, indicating that rock-derived cations
and unevenly distributed external inputs such as volcanic ashes are required to maintain C inputs and SOC. Importantly, our
results also emphasize that clay is not a reliable indicator for SOC content since our deeply weathered soils—which are typical
for large parts of the tropics—were dominated by low-activity clays with low reactive surface areas and thus limited potential
490   to stabilize SOC. Similarly, our study shows that SOC alone is not always a reliable indicator of soil fertility. For this reason,
we propose that a broader definition of soil fertility, that includes ECEC, is used when discussing highly weathered soils of
the humid tropics. Land degradation and subsequent abandonment in the mafic region did not seem to be related to SOC
content, but rather to nutrient limitations and Al mobility, which probably cause toxic conditions for plant growth. Importantly,
replanting abandoned fields with *Eucalyptus* monocultures did not lead to a substantial restoration of soil C stocks but instead
495   led to further depletion of critical soil nutrients. This finding undermines the idea of reforesting with non-native tree species in
order to generate a significant C sink in degraded, deeply weathered soils. The average estimated erosion rates of $0.5 \, \mathrm{cm \, yr^{-1}}$

resulted in a life span of croplands until field abandonment on sloping land in the region of 100–170 years after deforestation. Considering that most of the croplands in the region were cleared in the early 20th century, a period of further land abandonment threatening remaining forests is likely in upcoming years if agricultural practices remain as they are today. Our results give clear evidence of the severity of soil erosion in the region, which might cause threats for food security of a growing population in coming decades. More sustainable management and investments in supporting subsistence farmers to maintain fertile *kalongo* soils are needed today to avoid future crises across our study area and similar regions in tropical Eastern Africa.

Code and data availability. Code and data to reproduce the obtained results are available on the GitHub repository / Zenodo: laura-summerauer/soildeg-easternafrica-publication, https://doi.org/10.5281/zenodo.17157668.

Appendix A: Soil infrared spectroscopy for complementing conventional soil analyses

A1 Data acquisition and spectra processing

The pulverized samples were measured in duplicates on a VERTEX70 infrared spectrometer with a high-throughput screening extension (HTS-XT) (Bruker Optics GmbH, Germany). Instrument settings and sample handling followed the procedures described in Summerauer et al. (2021) used to develop the Central African Soil Infrared Library (CSSL). Each sample was measured with a resolution of $2\,cm^{-1}$ between 7500–$600\,cm^{-1}$ wavenumber range. A gold reference material was used as a reflectance standard. The final spectrum of each soil sample was obtained by averaging 32 co-added scans and adjusting for atmospheric CO_2 and H_2O using the OPUS software (BRUKER Optics GmbH, Germany). The measurement duplicates of each sample were averaged to obtain one single spectrum per sample. The spectra were trimmed to exclusively include the infrared region ranging from 4000 to $600\,cm^{-1}$, thereby discarding the near-infrared region, and were resampled at a resolution of $16\,cm^{-1}$.

A2 Selection of calibration samples

We developed quantitative infrared models to estimate soil properties for these sample sets. We used calibration samples from two existing soil spectral libraries, specifically the Central African Soil Spectral Library (CSSL, Summerauer et al. (2021), n = 79–1685) and the African Soil Information Service Soil Spectral Library (AfSIS SSL, Vågen et al. (2020, 2022), n = 3397; Table A1). To ensure that the resulting calibration dataset is comprehensive enough to cover the soil variability of all newly collected samples, a subset of these two new sample sets (present study and colluvial study) were measured with traditional wet chemistry methods (see section below) added to the calibration set (n = 234–429; Table A1).

These additional calibration samples were selected using the Kennard-Stone sampling algorithm (Kennard and Stone, 1969) on the principal component space of the soil infrared spectra. Samples that were similar to the ones already in the spectral libraries (CSSL and AfSIS SSL) were avoided during sampling (this was achieved using the "init" argument within the ken-

Stone function in the `prospectr` package of the R programming environment; see Stevens and Ramirez-Lopez (2024) for more details). Additionally, to allow a robust validation and avoid overfitting during model training, we grouped the calibration sampling by soil core to have either all samples of a core in the calibration or prediction set. The combination of all calibration
530   data (CSSL, AfSIS SSL and new measurements) will later be called the calibration set.

A3   Calibration modeling

Memory-based learning was used for calibration modeling. For this, the *k*-nearest neighbors search is used to subset the relevant samples to train the localized weighted average partial least squares regression model (see Summerauer et al. (2021), and Ramirez-Lopez et al. (2024) for more details). The maximum number of neighbors was set to 500, or if fewer samples
535   were available, to the maximum number of available observations in the reference dataset (combined library and new paired infrared data with paired wet chemistry data). For the search of the nearest neighbors, we used the moving window correlation dissimilarity (Ramirez-Lopez et al., 2024). Model validation was done using a grouped cross-validation, where we used soil cores from the same region in Eastern Africa from the CSSL and the new analyzed reference cores (n_{cores}, Table A1) as hold-out cores. We predicted each of the cores iteratively by keeping it out of the model training. R^2, Root mean square error (RMSE),
540   performance to the interquartile distance (Interquartile range / RMSE; RPIQ), and the mean error (bias) were calculated from all cross-validated hold-out predictions to give estimates of predictive accuracy. The final model was trained using MBL and all available calibration data (see Table A1 and section below).

To obtain clay, silt, and sand as fractions from a total of 100% we followed the additive log-ratio transformation (Odeh
545   et al., 2003). The data were back-transformed prior calculations of modeling performance statistics (for more details, see also Ramirez-Lopez et al. (2019)). Pre-processing was optimized by minimizing the reconstruction error of the prediction set calculated by projection models built by the extended infrared libraries, see Summerauer et al. (2021) for more details. The final selected pre-processing is listed in Table A1.

A4   Reference analyses

550   To train the calibration models we used the infrared and available wet chemistry data of all infrared libraries (CSSL and AfSIS), and extended the dataset with additional measurements on a subset of our sample set and for the subsequent calibration modeling (see section above; Table A1). When laboratory methods differed substantially in their methods, we performed a comparison of the methods on a subset of samples in order to ensure data quality (see Appendix B).

555   All our samples were free of carbonates (pH <= 6.5). Therefore, powdered aliquots were measured for SOC and TN using total (dry) combustion (Variocube, Elementar). SOC stocks (in $t\,ha^{-1}$) were calculated by using SOC content ($g\,kg^{-1}$) x bulk density ($g\,cm^{-3}$) x increment height (cm) x 0.1. Soil pH was measured on $2\,mm$ sieved samples in $0.01\,M$ CaCl$_2$ with a soil solution ratio of 1:5 and the pH value was determined using a Metrohm 713 pH Meter (Metrohm, Switzerland). Exchangeable cations (Al^{3+}, Mg^{2+}, Ca^{2+}, Na$^+$, K$^+$) were extracted on $2\,mm$ sieved material at soil pH using BaCl$_2$ as in Hendershot and

560   Duquette (1986). Cation contents in the $BaCl_2$ extraction were measured using inductively coupled plasma-optical emission spectroscopy (ICP-OES, 5100 ICP-OES Agilent Technologies, USA). The Effective cation exchange capacity (ECEC) was calculated as the sum of exchangeable Al^{3+}, Mg^{2+}, Ca^{2+}, Na^+, K^+, and H^+, where H^+ was calculated using $10^{-pH}x100$. Since Al^{3+} could not be modeled with the infrared spectra (low accuracies), it was estimated by ECEC - sum of bases - H^+ (for the prediction samples; i.e. samples with only infrared data). Pedogenic oxides were extracted from milled samples

565   using the multiple-step approach by Stucki et al. (1987): metal-organo complexes (Fe_{Py}, Al_{Py}) were extracted at pH 10 with sodium-pyrophosphate (Bascomb, 1968), and the amorphous secondary metals (Fe_{Ox}, Al_{Ox}) were extracted using ammonium oxalate-oxalic acid at pH 3 (Dahlgren, 1994); see also Reichenbach et al. (2021) for more details. We refer to the sum of both metal forms (Al_{PyOx} and Fe_{PyOx}) which represent the reactive metal fraction. The ratio Al_{Py}:Al_{Ox} indicates whether Al is bound to allophanes or in Al-humus complexes (Mizota and Reeuwijk, 1989). Soil texture was analyzed using the hydrometer

570   method (Bouyoucos, 1962) with the adjustments as suggested by Beretta et al. (2014): after dispersion in $10\,\%$ $(NaPO_3)_6$ and three applications of $6\,\%$ H_2O_2, silt ($2–53\,\mu m$) and clay ($< 2\,\mu m$) fractions were determined using the hydrometer readings at different time points. The sand fraction ($53–2000\,\mu m$) was separately determined by wet sieving, see Doetterl et al. (2021a, b) for more details.

Table A1. Soil properties, preprocessing of mid-infrared data prior to calibration modeling, number of available samples in existing libraries (n_{CSSL}, n_{AfSIS}), and new paired mid-infrared with reference data (n_{new}), and validation statistics of a grouped cross-validation (number of hold-out cores (n_{cores}), R^2, Root Means Square Error (RMSE), performance to the interquartile distance (RPIQ), mean error/bias). Preprocessing details: sg(m, p, w) = Savitzki-Golay filter with differentiation order, polynomial order, window size; msc = cultiplicative scatter correction.

Property	Pre-processing	n_{CSSL}	n_{AfSIS}	n_{new}	$n_{samples}$ / n_{cores}	R^2	RMSE	RPIQ	bias
		reference samples			5 grouped cross-validation				
SOC (g kg^{-1})	sg(2,2,17) + msc	1669	3397	234	484 / 92	0.9	5.45	3.6	-0.73
TN (g kg^{-1})	sg(1,3,9) + msc	1685	3397	234	484 / 92	0.9	0.45	3.44	-0.03
pH (-)	sg(2,2,7) + msc	513	-	429	635 / 150	0.73	0.44	2.86	-0.04
ECEC (cmol$_c$ kg^{-1})	sg(1,3,7) + msc	432	-	228	415 / 91	0.76	3.14	2.67	0.15
Sum of bases (cmol$_c$ kg^{-1})	sg(1,3,7) + msc	432	-	228	415 / 91	0.8	3.26	3.4	0.37
FePyOx (mass%)	sg(1,3,9) + msc	79*	-	-	79 / 24	0.54	0.62	2.09	-0.06
AlPyOx (mass%)	sg(2,2,17)	79*	-	-	79 / 24	0.74	0.14	3.15	0.01
AlOx (mass%)	sg(2,2,17)	79*	-	-	79 / 24	0.67	0.11	2.5	0
Clay <2 µm (%) **	sg(2,2,7) + msc	234*	-	-	234 / 77	0.86	6.3	3.99	-0.47
Silt 2–53 µm (%) **	sg(2,2,7) + msc	234*	-	-	234 / 77	0.72	4.62	1.85	0.2
Sand 53–2000 µm (%) **	sg(2,2,7) + msc	234*	-	-	234 / 77	0.79	7.33	3.35	0.27

*reference data TropSOC database only, ** back-transformed data.

Appendix B: Data merging between databases

575 Data for pH and exchangeable cations of the TropSOC database were measured with different methods and in a different laboratory (soil laboratory at the International Institute of Tropical Agriculture Kalambo, DRC). The compatibility of the both methods were assured by re-measuring samples at ETH Zurich using established methods (see section above). The method comparison for pH showed a high correlation to our obtained results with $CaCl_2$ to the KCl but a shift of 0.3 (linear regression: $pH_{ETH/CaCl_2} = 0.3 + pH_{IITA/KCl}$ with an $R^2 = 0.96$, $n = 10$, results not shown). Therefore, TropSOC pH data were bias corrected
580 by adding 0.3. Exchangeable cations (Mg^{2+}, Ca^{2+}, Na^+, K^+) were extracted at soil pH using NH_4Cl percolation and measured using flame photometry and atomic absorption spectrophotometry (Pauwels et al., 1992). Exchangeable Al^{3+} was measured with a titration using KCl, NaOH, and HCl (McLean, 1965). The effective cation exchange capacity was calculated with the sum of Al^{3+}, Mg^{2+}, Ca^{2+}, Na^+, K^+, and H^+, with $H^+ = 10^{-pH} x100$ (the calculation for H^+ was adjusted for consistency purposes in this study). The correlation of both methods resulted for ECEC in an R^2 of 0.97, the sum of exchangeable base cation in an
585 R^2 of 0.98, and for Al^{3+} an R^2 of 0.94, respectively ($n = 20$; results not shown). See Doetterl et al. (2021a, b) for more details on these methods.

Appendix C: Changes to soil pH and texture with time after deforestation

In topsoils of the mafic region, pH_{CaCl_2} ranged between 2.7–5.8 with lowest values in cropland topsoils 2–7 years after deforestation (mean: 3.3) and highest values in abandoned sites (mean: 4.5) (Figure D1). An increase of the mean values from
590 forests (4.0) to cropland (4.5) was observed on sites >60 years after deforestation. Topsoils under Eucalyptus monocultures had pH_{CaCl_2} values of 4.0 regardless of time since deforestation (Figure S1). In contrast, pH_{CaCl_2} in topsoils of the felsic region ranged between 4.2–6.5 independently of time since deforestation. Highest values were measured under forest (mean 5.6) and under cropland (mean values 5.1–5.3).

595 On mafic parent material, the texture of the topsoils (0–10 cm) was coarse under forest and on croplands of recently cleared sites (2–7, 10–20 years) (mean values: 32.6–37.7 % sand and 62.4–67.4 % fine soil texture (silt + clay); Figure D1). However, on cropland, abandoned, and Eucalyptus sites, which were cleared 40–60 and >60 years ago, the texture was finer (mean values: 20.3–29.6 % sand, 70.4–79.7 % silt + clay). Similar patterns were also observed in the felsic region, where topsoils were coarser under forest (54.4 % sand, 45.6 % silt + clay), and finer on sites which were cleared 40–60 and >60 years ago (26.0–38.4 %
600 sand, 61.6–74.0 % sit + clay), regardless of land use (except one site sampled under Eucalyptus, which was cleared >60 years ago, 45.5 % sand, 54.5 % silt + clay; Figure D1).

Appendix D: Additional graphs
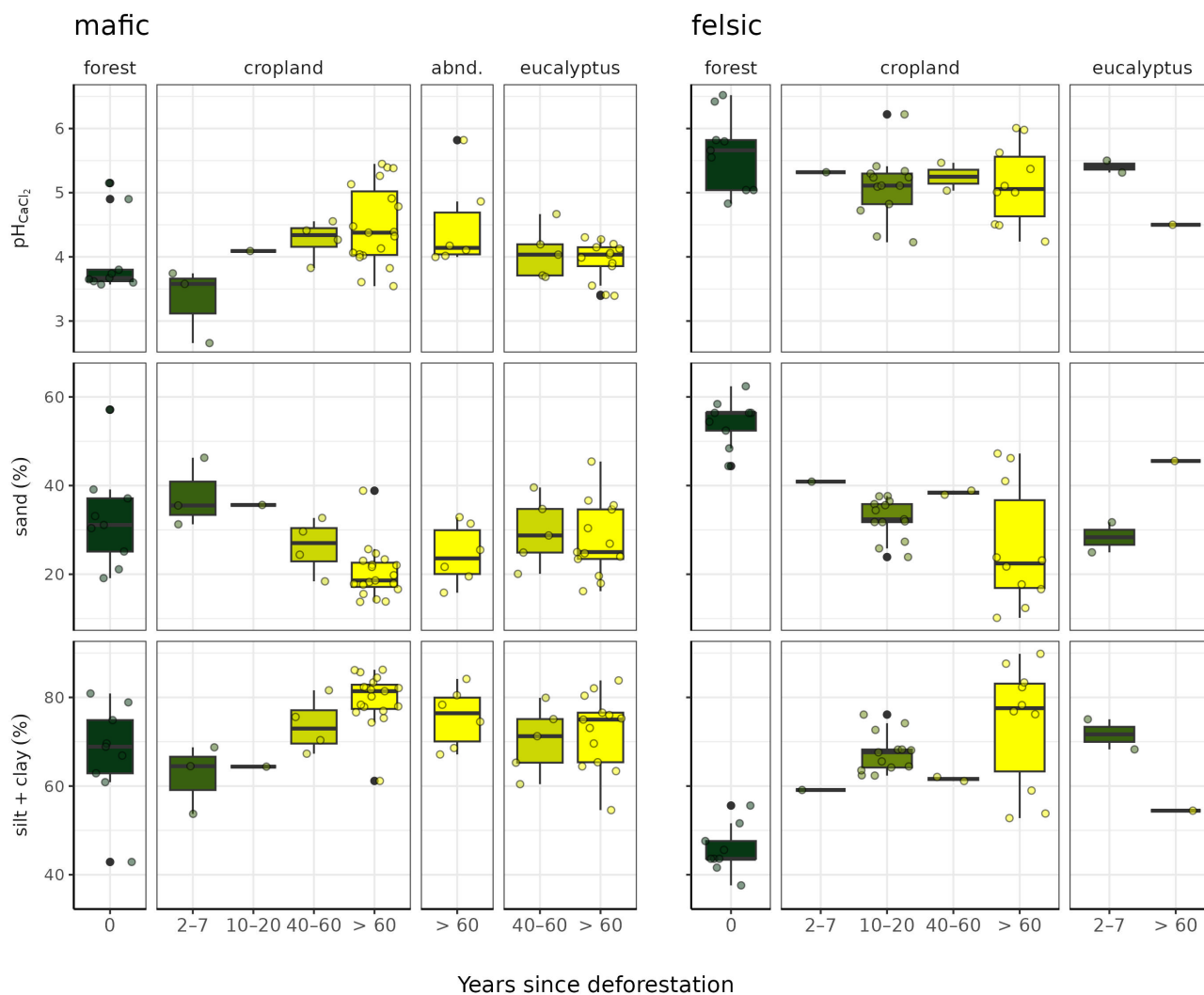
Figure D1. Changes in pH$_{CaCl_2}$, as well as fine soil texture (silt + clay) and sand along the deforestation chronosequence in topsoils (0–10 cm) developed on mafic (left) and felsic (right) parent material.
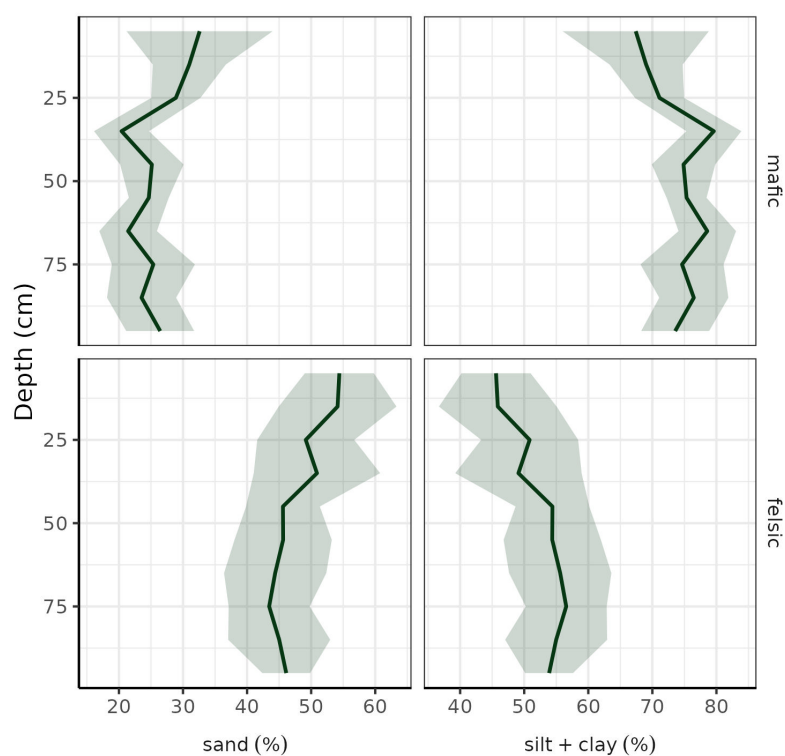
Figure D2. Particle sizes: sand (left) and fine soil texture (right) in old-growth and pristine forests in both geochemical regions (top: mafic, bottom: felsic) in a soil depth of 0–100 cm. Data source: TropSOC database (Doetterl et al., 2021a, b).
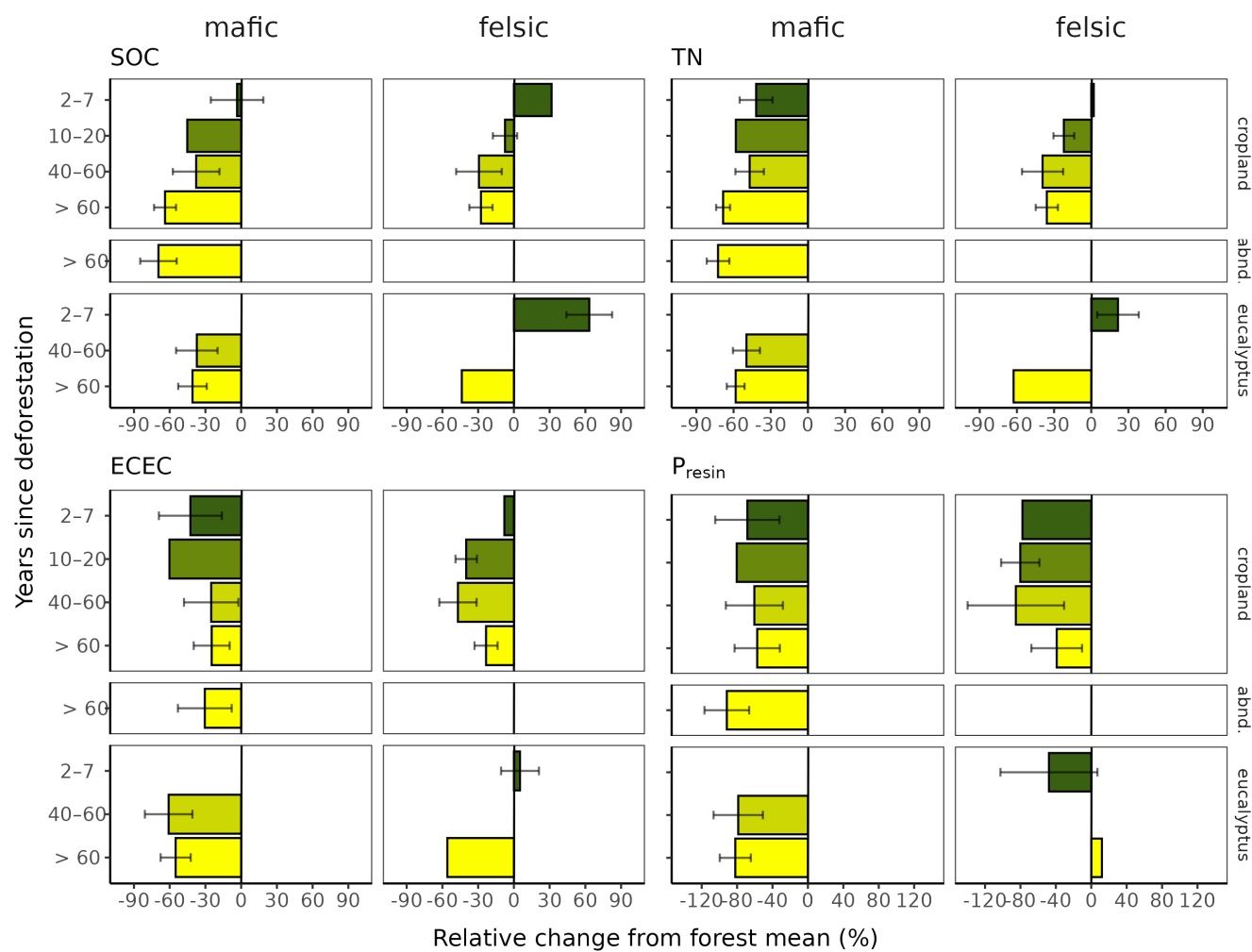
Figure D3. Relative change of soil organic carbon (SOC), total nitrogen (TN), effective cation exchange capacity (ECEC), and plant available P (P$_{resin}$) in hillslope topsoils compared to forest topsoils (0–10cm) along the deforestation chronosequence (0, 2–7, 10–20, 40–60, >60 years since deforestation) in soils developed on mafic and felsic parent material. Error bars are the standard errors of the mean of each group and the forest mean.
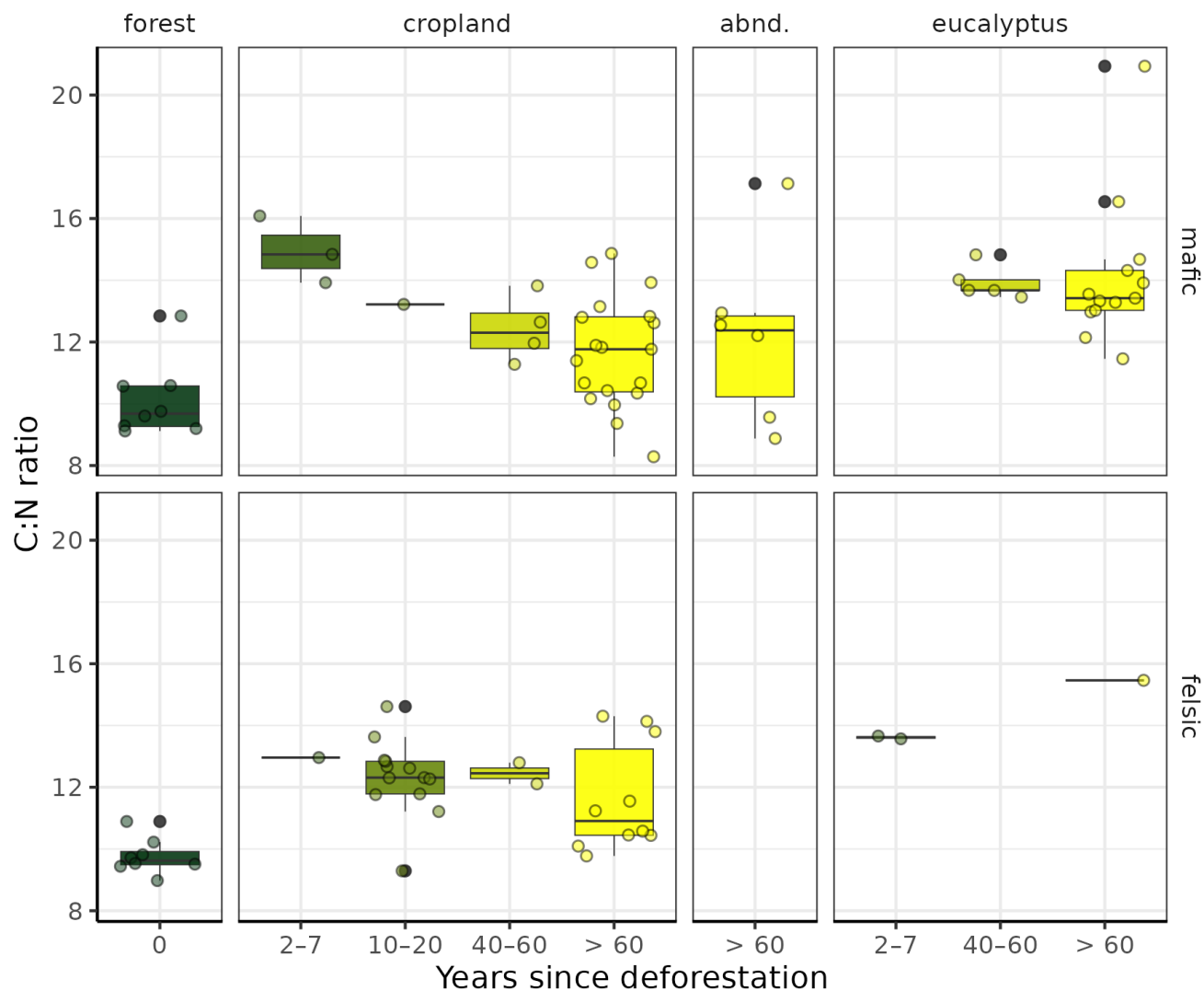
Figure D4. C:N ratio in 0–10 cm under forests, croplands, *Eucalyptus* and on abandoned sites (abnd.) along the deforestation chronosequence (0, 2–7, 10–20, 40–60, >60 years since deforestation) in soils developed on mafic (top) and felsic (bottom) parent material.
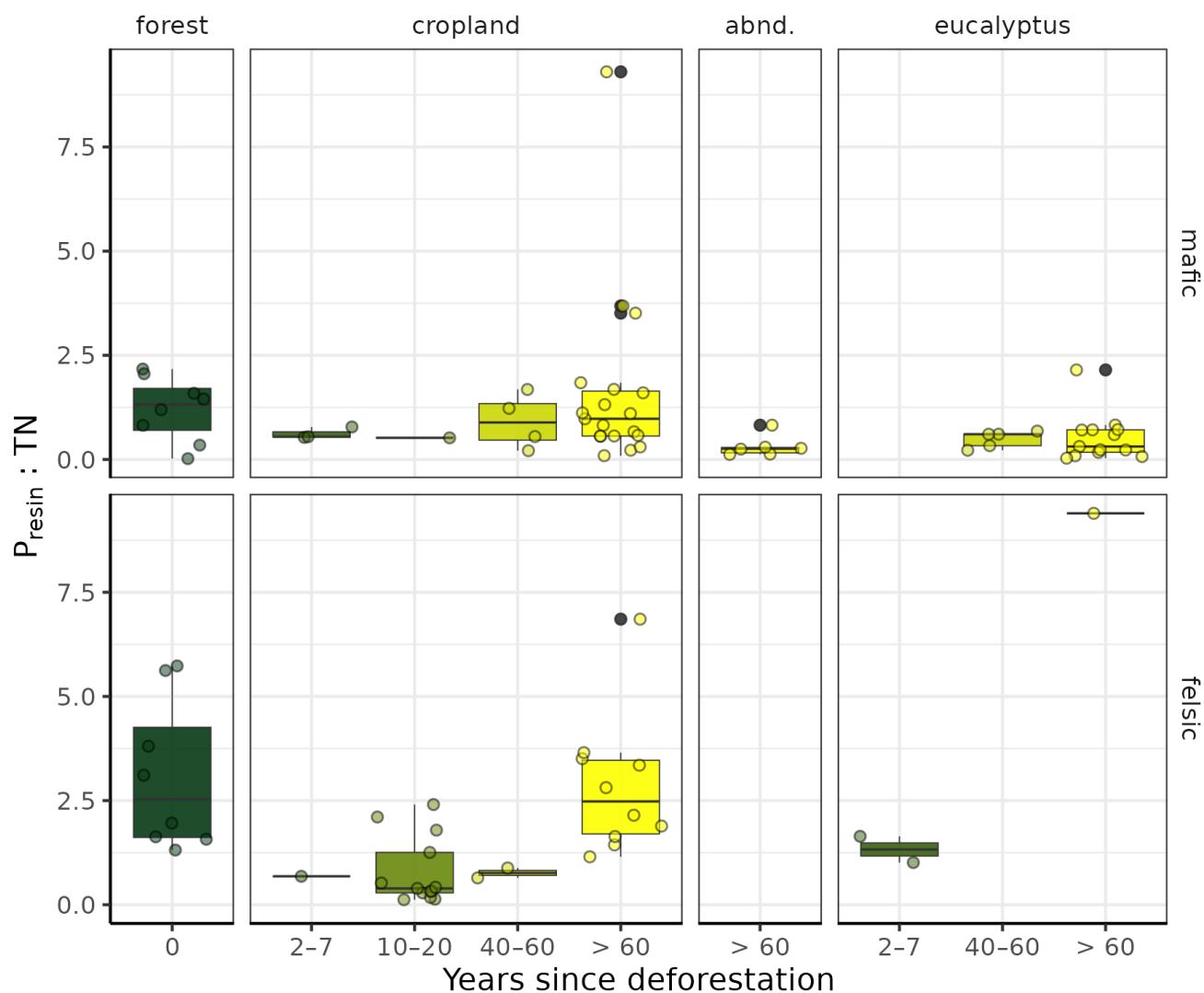
Figure D5. P_{resin}:TN ratio in 0–10 cm under forests, croplands, *Eucalyptus* and on abandoned sites (abnd.) along the deforestation chronosequence (0, 2–7, 10–20, 40–60, >60 years since deforestation) in soils developed on mafic (top) and felsic (bottom) parent material.
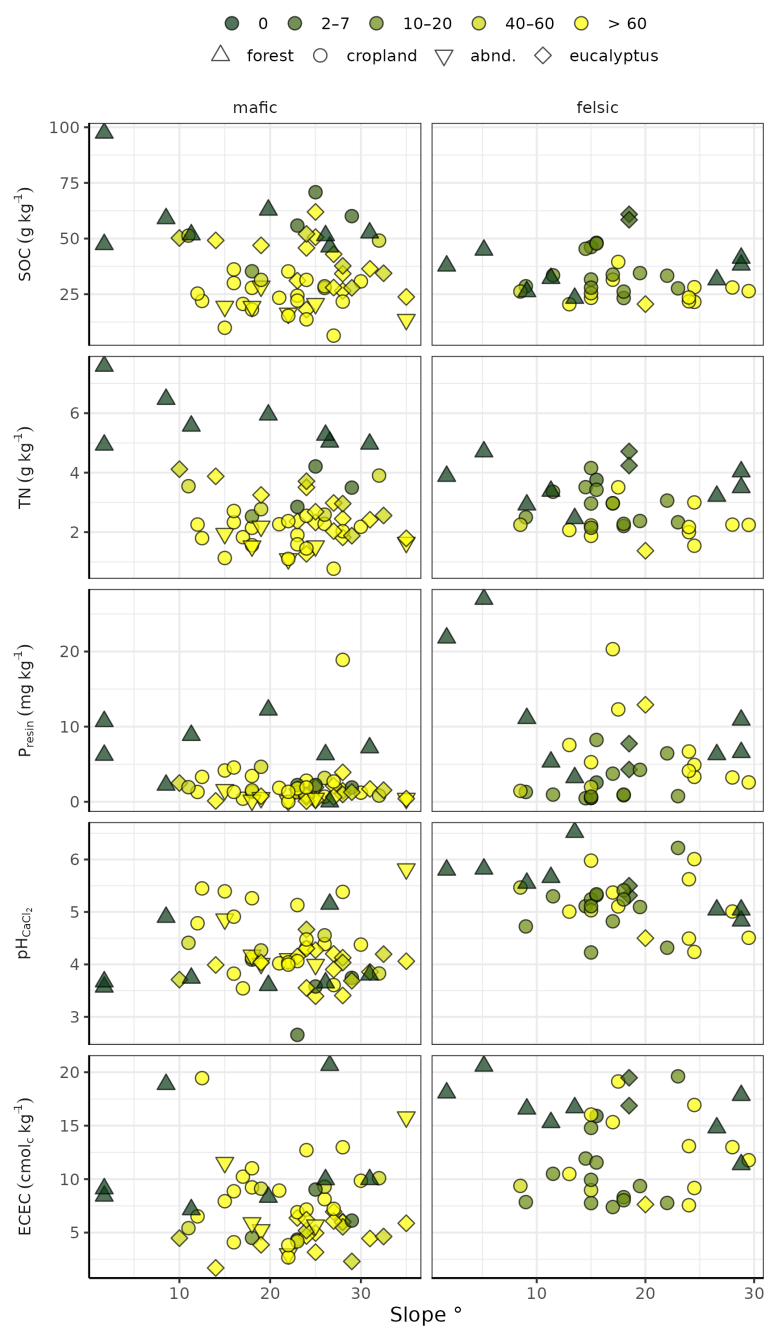
Figure D6. Slope angle in vs. soil organic carbon (SOC), total nitrogen (TN), bio-available P (P_{resin}), pH_{CaCl_2}, and effective cation exchange capacity (ECEC) in the two geochemical regions mafic (left) and felsic (right).
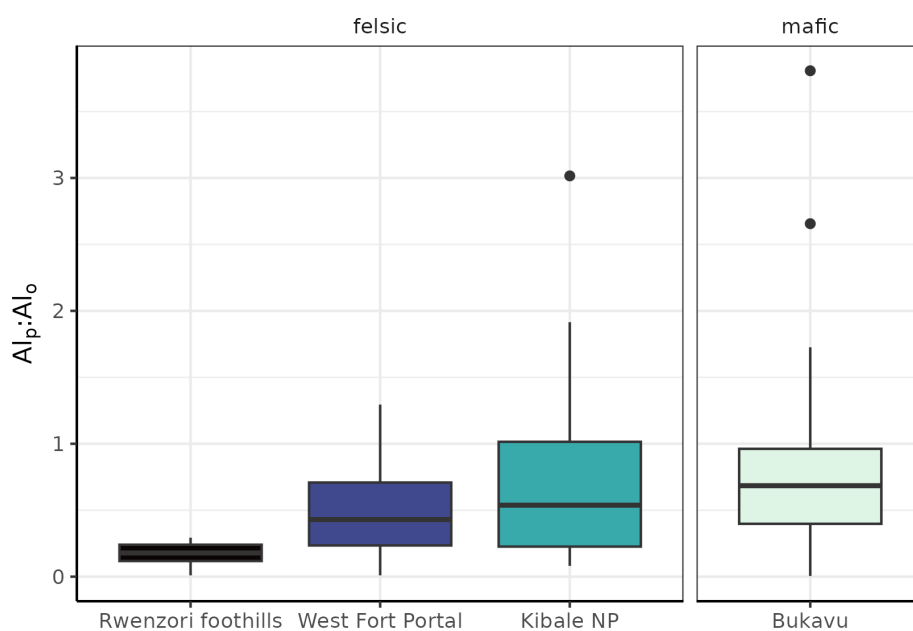
Figure D7. Pyrophosphate-extractable to oxalate-extractable aluminum ratio (Al_P:Al_O) over the regions in the two geochemical sampling regions. A ratio close to 0 indicates Al in allophanes, while a value close to 1 indicates Al-humus complexes (Mizota and Reeuwijk, 1989). Felsic sites: The Rwenzori foothills ($n = 6$) are located along the mountain chain Southwest of Fort Portal, West Fort Portal sites ($n = 23$) are located between 30.5 to 31.0° and 0.5 to 1°, Northwest of Fort Portal, while the Kibale NP ($n = 9$) are located in the National Park, south of Fort Portal. Mafic sites: The sites are located west of the city of Bukavu ($n = 60$), in South Kivu province, Democratic Republic of Congo.
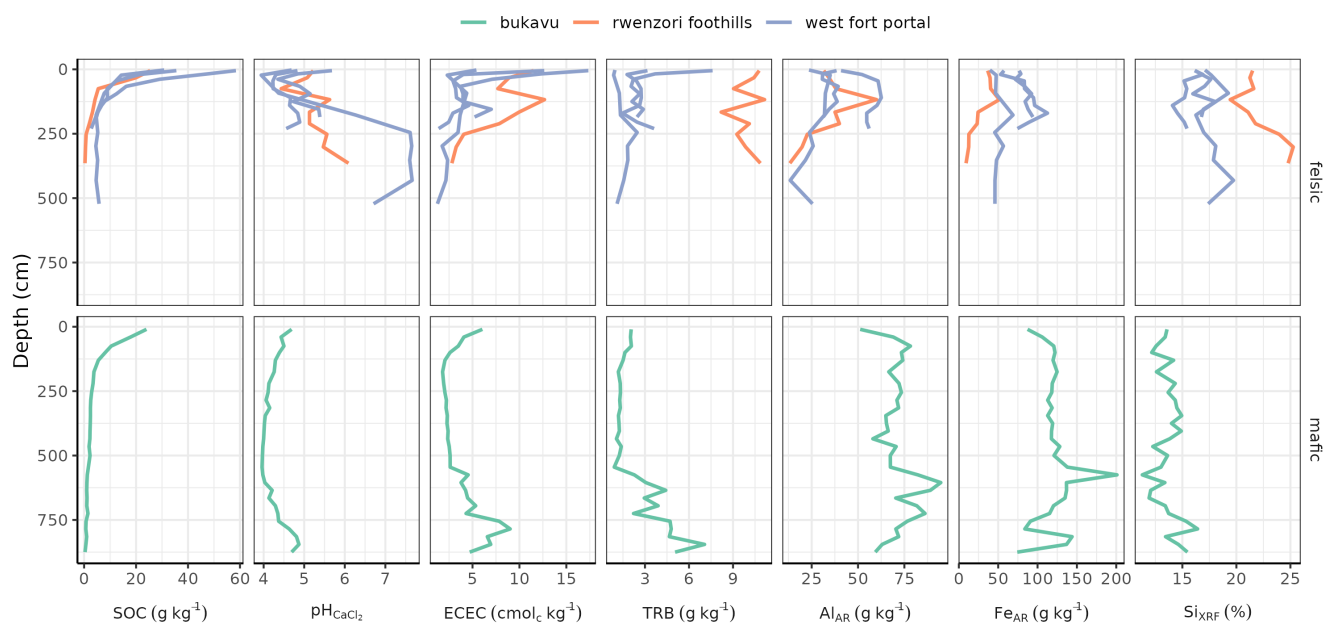
Figure D8. Soil profiles (felsic: road cuts; mafic: basalt mine), sampled down to the saprolite or to the bedrock.
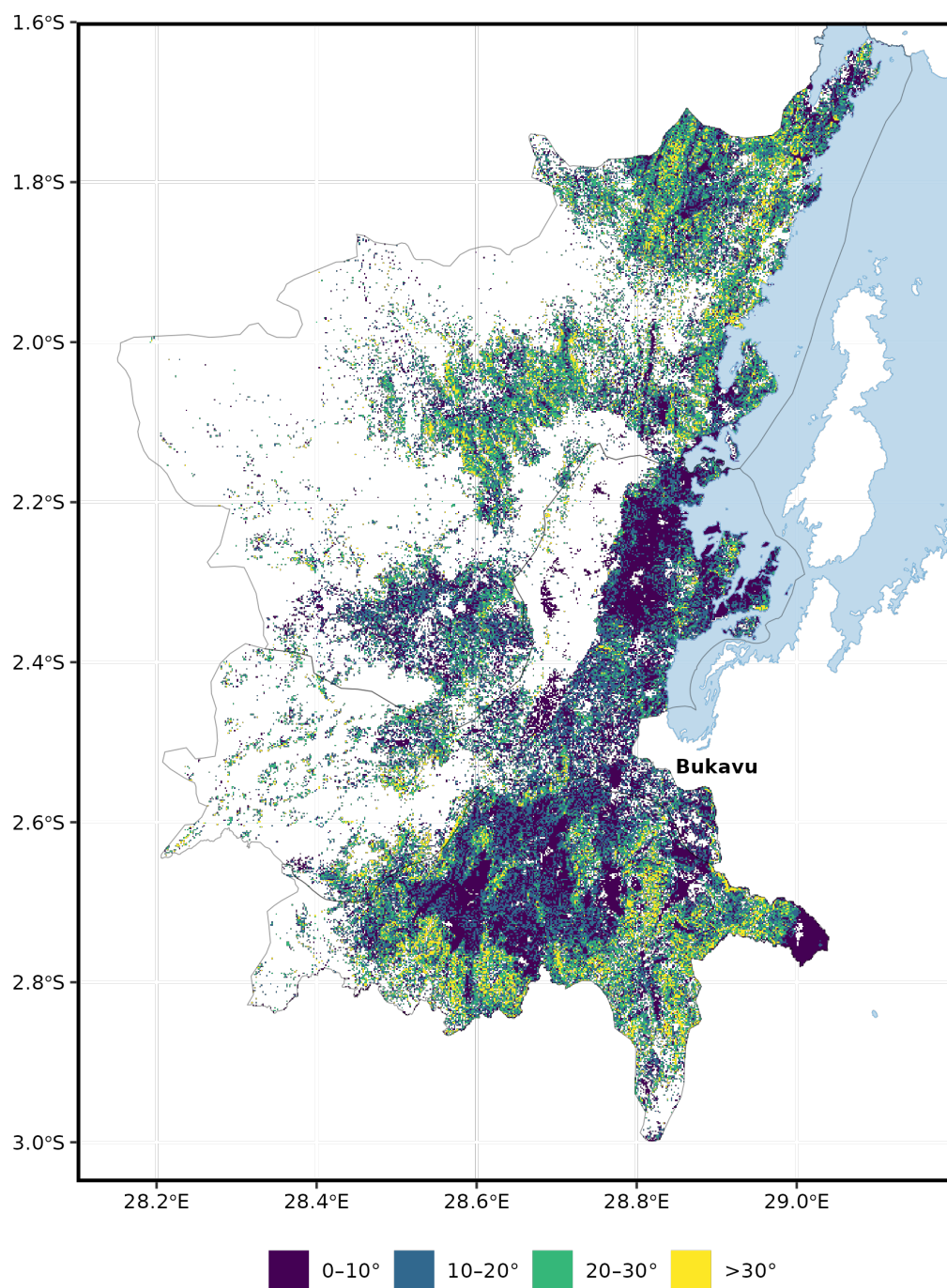
Figure D9. Slope inclination distributions on land (without forested, built-up areas, open water) in the three territories Walungu, Kabare, and Kalehe in the province South Kivu. Slope was calculated from a digital elevation model (SRTM 30 m), land cover information was used from ESA-CCI (ESA-CCI S2 prototype Land Cover 20 m map of Africa 2016)

Author contributions. SD, and LS have conceptualized the project and paper. SD designed the research. LS has led the research. LS, FB, DM, BA, and AW have selected the study sites, conducted the field work and led the coordination in the field. CK and LCN have provided crucial local facilities and information, LRL and LS have developed the soil analyses using infrared spectroscopy, LS has led all the laboratory work, performed all the statistical analyses and graphical visualizations. All authors contributed to the writing of the paper.

Competing interests. Marijn Bauters is an associate editor for Biogeosciences.

Acknowledgements. We are truly thankful to all the smallholder farmers in the Democratic Republic of Congo and Uganda who supported our sampling. We also express our gratitude to all field helpers and coordinators for their support. We acknowledge the Unviersité Catholique de Bukavu and Mountains of the Moon University for providing us with their facilities. We warmly thank Fabien Munzihirwa and Kadiri Mugenyi and the Soil Resources group at ETH Zurich for their support in the laboratory. We also thank Kristof van Oost, Matti Barthel, Oliver Chadwick, and the Congo Biogeochemistry Observatory for the inspiration.

References

Amundson, R., Berhe, A. A., Hopmans, J. W., Olson, C., Sztein, A. E., and Sparks, D. L.: Soil and human security in the 21st century, Science, 348, 1261 071, https://doi.org/10.1126/science.1261071, publisher: American Association for the Advancement of Science, 2015.

Angst, G., Messinger, J., Greiner, M., Häusler, W., Hertel, D., Kirfel, K., Kögel-Knabner, I., Leuschner, C., Rethemeyer, J., and Mueller, C. W.: Soil organic carbon stocks in topsoil and subsoil controlled by parent material, carbon input in the rhizosphere, and microbial-derived compounds, Soil Biology and Biochemistry, 122, 19–30, https://doi.org/10.1016/j.soilbio.2018.03.026, 2018.

Araujo, M. A., Zinn, Y. L., and Lal, R.: Soil parent material, texture and oxide contents have little effect on soil organic carbon retention in tropical highlands, Geoderma, 300, 1–10, https://doi.org/10.1016/j.geoderma.2017.04.006, 2017.

Augusto, L., Achat, D. L., Jonard, M., Vidal, D., and Ringeval, B.: Soil parent material—A major driver of plant nutrient limitations in terrestrial ecosystems, Global Change Biology, 23, 3808–3824, https://doi.org/10.1111/gcb.13691, _eprint: https://onlinelibrary.wiley.com/doi/pdf/10.1111/gcb.13691, 2017.

Authority, U. I.: Rwenzori Region, Agriculture Sector Investment Profile, Tech. rep., Uganda, https://www.ugandainvest.go.ug/wp-content/uploads/2020/11/Agriculture-Sector-Investment-Profile-Rwenzori-Region.pdf, 2020.

Bailey, K., Lloyd, F., Kearns, S., Stoppa, F., Eby, N., and Woolley, A.: Melilitite at Fort Portal, Uganda: Another dimension to the carbonate volcanism, Lithos, 85, 15–25, https://doi.org/10.1016/j.lithos.2005.03.019, 2005.

Bamwesigye, D., Chipfakacha, R., and Yeboah, E.: Forest and Land Rights at a Time of Deforestation and Climate Change: Land and Resource Use Crisis in Uganda, Land, 11, 2092, https://doi.org/10.3390/land11112092, 2022.

Barker, D. S. and Nixon, P. H.: High-Ca, low-alkali carbonatite volcanism at Fort Portal, Uganda, Contributions to Mineralogy and Petrology, 103, 166–177, https://doi.org/10.1007/BF00378502, 1989.

Bascomb, C. L.: Distribution of Pyrophosphate-Extractable Iron and Organic Carbon in Soils of Various Groups, Journal of Soil Science, 19, 251–268, https://doi.org/10.1111/j.1365-2389.1968.tb01538.x, _eprint: https://onlinelibrary.wiley.com/doi/pdf/10.1111/j.1365-2389.1968.tb01538.x, 1968.

Baumann, P., Knecht, T., and Roudier, P.: opusreader2: Read Spectroscopic Data from Bruker OPUS Binary Files. R package version 0.6.2.9000, https://github.com/spectral-cockpit/opusreader2, 2024.

Bauters, M., Drake, T. W., Verbeeck, H., Bodé, S., Hervé-Fernández, P., Zito, P., Podgorski, D. C., Boyemba, F., Makelele, I., Cizungu Ntaboba, L., Spencer, R. G. M., and Boeckx, P.: High fire-derived nitrogen deposition on central African forests, Proceedings of the National Academy of Sciences, 115, 549–554, https://doi.org/10.1073/pnas.1714597115, publisher: Proceedings of the National Academy of Sciences, 2018.

Bauters, M., Drake, T. W., Wagner, S., Baumgartner, S., Makelele, I. A., Bodé, S., Verheyen, K., Verbeeck, H., Ewango, C., Cizungu, L., Van Oost, K., and Boeckx, P.: Fire-derived phosphorus fertilization of African tropical forests, Nature Communications, 12, 5129, https://doi.org/10.1038/s41467-021-25428-3, number: 1 Publisher: Nature Publishing Group, 2021.

Bauters, M., Janssens, I. A., Wasner, D., Doetterl, S., Vermeir, P., Griepentrog, M., Drake, T. W., Six, J., Barthel, M., Baumgartner, S., Van Oost, K., Makelele, I. A., Ewango, C., Verheyen, K., and Boeckx, P.: Increasing calcium scarcity along Afrotropical forest succession, Nature Ecology & Evolution, 6, 1122–1131, https://doi.org/10.1038/s41559-022-01810-2, publisher: Nature Publishing Group, 2022.

Beretta, A. N., Silbermann, A. V., Paladino, L., Torres, D., Bassahun, D., Musselli, R., and García-Lamohte, A.: Soil texture analyses using a hydrometer: modification of the Bouyoucos method, Ciencia e investigación agraria, 41, 263–271, https://doi.org/10.4067/S0718-16202014000200013, 2014.

650 Berhe, A. A., Harte, J., Harden, J. W., and Torn, M. S.: The Significance of the Erosion-induced Terrestrial Carbon Sink, BioScience, 57, 337–346, https://doi.org/10.1641/B570408, 2007.

Bertrand, I., Viaud, V., Daufresne, T., Pellerin, S., and Recous, S.: Stoichiometry constraints challenge the potential of agroecological practices for the soil C storage. A review, Agronomy for Sustainable Development, 39, 54, https://doi.org/10.1007/s13593-019-0599-6, 2019.

Blume, H.-P., Brümmer, G. W., Fleige, H., Horn, R., Kandeler, E., Kögel-Knabner, I., Kretzschmar, R., Stahr, K., and Wilke, B.-M.: Inorganic
655 Soil Components—Minerals and Rocks, in: Scheffer / Schachtschabel Soil Science, edited by Blume, H.-P., Brümmer, G. W., Fleige, H., Horn, R., Kandeler, E., Kögel-Knabner, I., Kretzschmar, R., Stahr, K., and Wilke, B.-M., pp. 7–53, Springer, Berlin, Heidelberg, ISBN 978-3-642-30942-7, https://doi.org/10.1007/978-3-642-30942-7_2, 2016.

Bouillet, J.-P., Laclau, J.-P., Gonçalves, J. L. d. M., Voigtlaender, M., Gava, J. L., Leite, F. P., Hakamada, R., Mareschal, L., Mabiala, A., Tardy, F., Levillain, J., Deleporte, P., Epron, D., and Nouvellon, Y.: *Eucalyptus* and *Acacia* tree growth over entire rota-
660 tion in single- and mixed-species plantations across five sites in Brazil and Congo, Forest Ecology and Management, 301, 89–101, https://doi.org/10.1016/j.foreco.2012.09.019, 2013.

Bouyoucos, G. J.: Hydrometer Method Improved for Making Particle Size Analyses of Soils1, Agronomy Journal, 54, 464–465, https://doi.org/10.2134/agronj1962.00021962005400050028x, _eprint: https://onlinelibrary.wiley.com/doi/pdf/10.2134/agronj1962.00021962005400050028x, 1962.

665 Brancalion, P. H. S., Amazonas, N. T., Chazdon, R. L., van Melis, J., Rodrigues, R. R., Silva, C. C., Sorrini, T. B., and Holl, K. D.: Exotic eucalypts: From demonized trees to allies of tropical forest restoration?, Journal of Applied Ecology, 57, 55–66, https://doi.org/10.1111/1365-2664.13513, _eprint: https://onlinelibrary.wiley.com/doi/pdf/10.1111/1365-2664.13513, 2020.

Bristow, C. S., Hudson-Edwards, K. A., and Chappell, A.: Fertilizing the Amazon and equatorial Atlantic with West African dust, Geophysical Research Letters, 37, https://doi.org/10.1029/2010GL043486, _eprint:
670 https://onlinelibrary.wiley.com/doi/pdf/10.1029/2010GL043486, 2010.

Bruun, T. B., Elberling, B., and Christensen, B. T.: Lability of soil organic carbon in tropical soils with different clay minerals, Soil Biology and Biochemistry, 42, 888–895, https://doi.org/10.1016/j.soilbio.2010.01.009, 2010.

Bukombe, B., Bauters, M., Boeckx, P., Cizungu, L. N., Cooper, M., Fiener, P., Kidinda, L. K., Makelele, I., Muhindo, D. I., Rewald, B., Verheyen, K., and Doetterl, S.: Soil geochemistry – and not topography – as a major driver of carbon allocation, stocks, and dynamics in
675 forests and soils of African tropical montane ecosystems, New Phytologist, 236, 1676–1690, https://doi.org/10.1111/nph.18469, _eprint: https://onlinelibrary.wiley.com/doi/pdf/10.1111/nph.18469, 2022.

Chadwick, K. D. and Asner, G. P.: Tropical soil nutrient distributions determined by biotic and hillslope processes, Biogeochemistry, 127, 273–289, https://doi.org/10.1007/s10533-015-0179-z, 2016.

Coleman, K. and Jenkinson, D. S.: RothC-26.3 - A Model for the turnover of carbon in soil, in: Evaluation of Soil Organic Matter Models,
680 edited by Powlson, D. S., Smith, P., and Smith, J. U., NATO ASI Series, pp. 237–246, Springer, Berlin, Heidelberg, ISBN 978-3-642-61094-3, https://doi.org/10.1007/978-3-642-61094-3_17, 1996.

Cook, R. L., Binkley, D., and Stape, J. L.: Eucalyptus plantation effects on soil carbon after 20years and three rotations in Brazil, Forest Ecology and Management, 359, 92–98, https://doi.org/10.1016/j.foreco.2015.09.035, 2016.

Cox, T. P.: Farming the battlefield: the meanings of war, cattle and soil in South Kivu, Democratic Republic of the Congo, Dis-
685 asters, 36, 233–248, https://doi.org/10.1111/j.1467-7717.2011.01257.x, _eprint: https://onlinelibrary.wiley.com/doi/pdf/10.1111/j.1467-7717.2011.01257.x, 2012.

Dahlgren, R. A.: Quantification of Allophane and Imogolite, in: Quantitative Methods in Soil Mineralogy, pp. 430–451, John Wiley & Sons, Ltd, ISBN 978-0-89118-884-1, https://doi.org/10.2136/1994.quantitativemethods.c14, section: 14 _eprint: https://onlinelibrary.wiley.com/doi/pdf/10.2136/1994.quantitativemethods.c14, 1994.

690   Davidson, E. A. and Ackerman, I. L.: Changes in soil carbon inventories following cultivation of previously untilled soils, Biogeochemistry, 20, 161–193, https://doi.org/10.1007/BF00000786, 1993.

Dechert, G., Veldkamp, E., and Anas, I.: Is soil degradation unrelated to deforestation? Examining soil parameters of land use systems in upland Central Sulawesi, Indonesia, Plant and Soil, 265, 197–209, https://doi.org/10.1007/s11104-005-0885-8, 2004.

Delcamp, A., Mossoux, S., Belkus, H., Tweheyo, C., Mattsson, H., and Kervyn, M.: Control of the stress field and rift structures on the
695   distribution and morphology of explosive volcanic craters in the Manyara and Albertine rifts, Journal of African Earth Sciences, 150, 566–583, https://doi.org/10.1016/j.jafrearsci.2018.09.012, 2019.

Depicker, A., Jacobs, L., Delvaux, D., Havenith, H.-B., Maki Mateso, J.-C., Govers, G., and Dewitte, O.: The added value of a regional landslide susceptibility assessment: The western branch of the East African Rift, Geomorphology, 353, 106 886, https://doi.org/10.1016/j.geomorph.2019.106886, 2020.

700   Depicker, A., Jacobs, L., Mboga, N., Smets, B., Van Rompaey, A., Lennert, M., Wolff, E., Kervyn, F., Michellier, C., Dewitte, O., and Govers, G.: Historical dynamics of landslide risk from population and forest-cover changes in the Kivu Rift, Nature Sustainability, 4, 965–974, https://doi.org/10.1038/s41893-021-00757-9, 2021.

Detwiler, R. P.: Land use change and the global carbon cycle: the role of tropical soils, Biogeochemistry, 2, 67–93, https://doi.org/10.1007/BF02186966, 1986.

705   Dick, D. P., Nunes Gonçalves, C., Dalmolin, R. S. D., Knicker, H., Klamt, E., Kögel-Knabner, I., Simões, M. L., and Martin-Neto, L.: Characteristics of soil organic matter of different Brazilian Ferralsols under native vegetation as a function of soil depth, Geoderma, 124, 319–333, https://doi.org/10.1016/j.geoderma.2004.05.008, 2005.

Doetterl, S., Cornelis, J.-T., Six, J., Bodé, S., Opfergelt, S., Boeckx, P., and Van Oost, K.: Soil redistribution and weathering controlling the fate of geochemical and physical carbon stabilization mechanisms in soils of an eroding landscape, Biogeosciences, 12, 1357–1371,
710   https://doi.org/10.5194/bg-12-1357-2015, doetterl_soilredr_2015, 2015.

Doetterl, S., Berhe, A. A., Arnold, C., Bodé, S., Fiener, P., Finke, P., Fuchslueger, L., Griepentrog, M., Harden, J. W., Nadeu, E., Schnecker, J., Six, J., Trumbore, S., Van Oost, K., Vogel, C., and Boeckx, P.: Links among warming, carbon and microbial dynamics mediated by soil mineral weathering, Nature Geoscience, 11, 589–593, https://doi.org/10.1038/s41561-018-0168-7, number: 8 Publisher: Nature Publishing Group, 2018.

715   Doetterl, S., Asifiwe, R. K., Baert, G., Bamba, F., Bauters, M., Boeckx, P., Bukombe, B., Cadisch, G., Cooper, M., Cizungu, L. N., Hoyt, A., Kabaseke, C., Kalbitz, K., Kidinda, L., Maier, A., Mainka, M., Mayrock, J., Muhindo, D., Mujinya, B. B., Mukotanyi, S. M., Nabahungu, L., Reichenbach, M., Rewald, B., Six, J., Stegmann, A., Summerauer, L., Unseld, R., Vanlauwe, B., Van Oost, K., Verheyen, K., Vogel, C., Wilken, F., and Fiener, P.: Organic matter cycling along geochemical, geomorphic, and disturbance gradients in forest and cropland of the African Tropics – project TropSOC database version 1.0, Earth System Science Data, 13, 4133–4153, https://doi.org/10.5194/essd-
720   13-4133-2021, publisher: Copernicus GmbH, 2021a.

Doetterl, S., Bukombe, B., Cooper, M., Kidinda, L., Muhindo, D., Reichenbach, M., Stegmann, A., Summerauer, L., Wilken, F., and Fiener, P.: TropSOC Database V 1.1, https://doi.org/10.5880/FIDGEO.2021.009, 2021b.

Don, A., Schumacher, J., and Freibauer, A.: Impact of tropical land-use change on soil organic carbon stocks – a meta-analysis, Global Change Biology, 17, 1658–1670, https://doi.org/10.1111/j.1365-2486.2010.02336.x, _eprint: https://onlinelibrary.wiley.com/doi/pdf/10.1111/j.1365-2486.2010.02336.x, 2011.

Drake, T. W., Van Oost, K., Barthel, M., Bauters, M., Hoyt, A. M., Podgorski, D. C., Six, J., Boeckx, P., Trumbore, S. E., Cizungu Ntaboba, L., and Spencer, R. G. M.: Mobilization of aged and biolabile soil carbon by tropical deforestation, Nature Geoscience, 12, 541–546, https://doi.org/10.1038/s41561-019-0384-9, number: 7 Publisher: Nature Publishing Group, 2019.

Duncan, A. J., Bachewe, F., Mekonnen, K., Valbuena, D., Rachier, G., Lule, D., Bahta, M., and Erenstein, O.: Crop residue allocation to livestock feed, soil improvement and other uses along a productivity gradient in Eastern Africa, Agriculture, Ecosystems & Environment, 228, 101–110, https://doi.org/10.1016/j.agee.2016.05.011, 2016.

D'Angelo, E., Crutchfield, J., and Vandiviere, M.: Rapid, Sensitive, Microscale Determination of Phosphate in Water and Soil, J. ENVIRON. QUAL., 30, 5, 2001.

Eufrade Junior, H. J., Melo, R. X. d., Sartori, M. M. P., Guerra, S. P. S., and Ballarin, A. W.: Sustainable use of eucalypt biomass grown on short rotation coppice for bioenergy, Biomass and Bioenergy, 90, 15–21, https://doi.org/10.1016/j.biombioe.2016.03.037, 2016.

Fialho, R. C. and Zinn, Y. L.: Changes in Soil Organic Carbon Under Eucalyptus Plantations in Brazil: A Comparative Analysis, Land Degradation & Development, 25, 428–437, https://doi.org/10.1002/ldr.2158, _eprint: https://onlinelibrary.wiley.com/doi/pdf/10.1002/ldr.2158, 2014.

Fiantis, D., Ginting, F. I., Gusnidar, Nelson, M., and Minasny, B.: Volcanic Ash, Insecurity for the People but Securing Fertile Soil for the Future, Sustainability, 11, 3072, https://doi.org/10.3390/su11113072, number: 11 Publisher: Multidisciplinary Digital Publishing Institute, 2019.

Fick, S. E. and Hijmans, R. J.: WorldClim 2: new 1-km spatial resolution climate surfaces for global land areas, International Journal of Climatology, 37, 4302–4315, https://doi.org/10.1002/joc.5086, 2017.

Gachuruzi, S. B.: The Impact of Refugees on the Environment: The Case of Rwandan Refugees in Kivu, Zaïre, Refuge: Canada's Journal on Refugees / Refuge: Revue canadienne sur les réfugiés, 15, 24–26, https://www.jstor.org/stable/45411513, publisher: Centre for Refugee Studies, York University, 1996.

Giller, K. E., Witter, E., Corbeels, M., and Tittonell, P.: Conservation agriculture and smallholder farming in Africa: The heretics' view, Field Crops Research, 114, 23–34, https://doi.org/10.1016/j.fcr.2009.06.017, 2009.

Guedes, B. S., Olsson, B. A., and Karltun, E.: Effects of 34-year-old Pinus taeda and Eucalyptus grandis plantations on soil carbon and nutrient status in former miombo forest soils, Global Ecology and Conservation, 8, 190–202, https://doi.org/10.1016/j.gecco.2016.09.005, 2016.

Guo, L. B. and Gifford, R. M.: Soil carbon stocks and land use change: a meta analysis, Global Change Biology, 8, 345–360, https://doi.org/10.1046/j.1354-1013.2002.00486.x, _eprint: https://onlinelibrary.wiley.com/doi/pdf/10.1046/j.1354-1013.2002.00486.x, 2002.

Hall, S. J. and Thompson, A.: What do relationships between extractable metals and soil organic carbon concentrations mean?, Soil Science Society of America Journal, 86, 195–208, https://doi.org/10.1002/saj2.20343, 2022.

Hansen, M. C., Potapov, P. V., Moore, R., Hancher, M., Turubanova, S. A., Tyukavina, A., Thau, D., Stehman, S. V., Goetz, S. J., Loveland, T. R., Kommareddy, A., Egorov, A., Chini, L., Justice, C. O., and Townshend, J. R. G.: High-Resolution Global Maps of 21st-Century Forest Cover Change, Science, 342, 850–853, https://doi.org/10.1126/science.1244693, 2013.

760 Harper, R. J., Okom, A. E. A., Stilwell, A. T., Tibbett, M., Dean, C., George, S. J., Sochacki, S. J., Mitchell, C. D., Mann, S. S., and Dods, K.: Reforesting degraded agricultural landscapes with *Eucalypts*: Effects on carbon storage and soil fertility after 26 years, Agriculture, Ecosystems & Environment, 163, 3–13, https://doi.org/10.1016/j.agee.2012.03.013, 2012.

Hedin, L. O., Vitousek, P. M., and Matson, P. A.: Nutrient Losses Over Four Million Years of Tropical Forest Development, Ecology, 84, 2231–2255, https://doi.org/10.1890/02-4066, _eprint: https://onlinelibrary.wiley.com/doi/pdf/10.1890/02-4066, 2003.

765 Hedley, M. J., Stewart, J. W. B., and Chauhan, B. S.: Changes in Inorganic and Organic Soil Phosphorus Fractions Induced by Cultivation Practices and by Laboratory Incubations, Soil Science Society of America Journal, 46, 970–976, https://doi.org/10.2136/sssaj1982.03615995004600050017x, _eprint: https://onlinelibrary.wiley.com/doi/pdf/10.2136/sssaj1982.03615995004600050017x, 1982.

Hendershot, W. H. and Duquette, M.: A Simple Barium Chloride Method for Determining Cation Exchange Capacity and Exchangeable
770 Cations, Soil Science Society of America Journal, 50, 605–608, https://doi.org/10.2136/sssaj1986.03615995005000030013x, _eprint: https://onlinelibrary.wiley.com/doi/pdf/10.2136/sssaj1986.03615995005000030013x, 1986.

Heri-Kazi, A. B. and Bielders, C. L.: Cropland characteristics and extent of soil loss by rill and gully erosion in smallholder farms in the KIVU highlands, D.R. Congo, Geoderma Regional, 26, e00 404, https://doi.org/10.1016/j.geodrs.2021.e00404, 2021.

Hijmans, R. J.: terra: Spatial Data Analysis. R package version 1.7-74, https://rspatial.github.io/terra/, 2024.

775 Hijmans, R. J., Barbosa, M., Ghosh, A., and Mandel, A.: geodata: Download Geographic Data. R package version 0.5-9, https://CRAN. R-project.org/package=geodata, 2024.

Hombegowda, H. C., van Straaten, O., Köhler, M., and Hölscher, D.: On the rebound: soil organic carbon stocks can bounce back to near forest levels when agroforests replace agriculture in southern India, SOIL, 2, 13–23, https://doi.org/10.5194/soil-2-13-2016, publisher: Copernicus GmbH, 2016.

780 Jacobs, L., Dewitte, O., Poesen, J., Maes, J., Mertens, K., Sekajugo, J., and Kervyn, M.: Landslide characteristics and spatial distribution in the Rwenzori Mountains, Uganda, Journal of African Earth Sciences, 134, 917–930, https://doi.org/10.1016/j.jafrearsci.2016.05.013, 2017.

Jagadamma, S., Lal, R., Ussiri, D. A. N., Trumbore, S. E., and Mestelan, S.: Evaluation of structural chemistry and isotopic signatures of refractory soil organic carbon fraction isolated by wet oxidation methods, Biogeochemistry, 98, 29–44, https://doi.org/10.1007/s10533-
785 009-9374-0, 2010.

Jagger, P. and Pender, J.: The role of trees for sustainable management of less-favored lands: the case of eucalyptus in Ethiopia, Forest Policy and Economics, 5, 83–95, https://doi.org/10.1016/S1389-9341(01)00078-8, 2003.

Jenny, H.: Factors of soil formation: a system of quantitative pedology, Dover books on earth sciences, Dover Publ, New York, unabridged, unaltered republ., new foreword edn., ISBN 978-0-486-68128-3, 1994.

790 Jobbágy, E. G. and Jackson, R. B.: Patterns and mechanisms of soil acidification in the conversion of grasslands to forests, Biogeochemistry, 64, 205–229, https://doi.org/10.1023/A:1024985629259, 2003.

Jones, A., Breuning-Madsen, H., Brossard, M., Dampha, A., Deckers, J., Dewitte, O., Hallett, S., Jones, R., Kilasara, M., Le Roux, P., Micheli, E., Montanarella, L., Spaargaren, O., Tahar, G., Thiombiano, L., Van Ranst, E., Yemefack, M., and Zougmore, R.: Soil Atlas of Africa, European Commission, Publication Office of the European Union, Luxembourg, ISBN 978-92-79-26715-4, https://doi.org/10.2788/52319,
795 2013.

Kallenbach, C. M., Frey, S. D., and Grandy, A. S.: Direct evidence for microbial-derived soil organic matter formation and its ecophysiological controls, Nature Communications, 7, 13 630, https://doi.org/10.1038/ncomms13630, number: 1 Publisher: Nature Publishing Group, 2016.

Kampunzu, A. B., Bonhomme, M. G., and Kanika, M.: Geochronology of volcanic rocks and evolution of the Cenozoic Western Branch of the East African Rift System, Journal of African Earth Sciences, 26, 441–461, https://doi.org/10.1016/S0899-5362(98)00025-6, 1998.

Kangela Matazi, A., Kany Luganda, E., and Mugisho Mukotanyi, S.: Does *Eucalyptus* determine agricultural soil quality?, Cogent Food & Agriculture, 9, 2157 115, https://doi.org/10.1080/23311932.2022.2157115, 2023.

Karamage, F., Shao, H., Chen, X., Ndayisaba, F., Nahayo, L., Kayiranga, A., Omifolaji, J. K., Liu, T., and Zhang, C.: Deforestation Effects on Soil Erosion in the Lake Kivu Basin, D.R. Congo-Rwanda, Forests, 7, 281, https://doi.org/10.3390/f7110281, number: 11 Publisher: Multidisciplinary Digital Publishing Institute, 2016.

Karamage, F., Zhang, C., Liu, T., Maganda, A., and Isabwe, A.: Soil Erosion Risk Assessment in Uganda, Forests, 8, 52, https://doi.org/10.3390/f8020052, number: 2 Publisher: Multidisciplinary Digital Publishing Institute, 2017.

Kennard, R. W. and Stone, L. A.: Computer Aided Design of Experiments, Technometrics, 11, 137–148, https://doi.org/10.1080/00401706.1969.10490666, 1969.

Kirsten, M., Mikutta, R., Vogel, C., Thompson, A., Mueller, C. W., Kimaro, D. N., Bergsma, H. L. T., Feger, K.-H., and Kalbitz, K.: Iron oxides and aluminous clays selectively control soil carbon storage and stability in the humid tropics, Scientific Reports, 11, 5076, https://doi.org/10.1038/s41598-021-84777-7, 2021.

Klinge, R., Araujo Martins, A., Mackensen, J., and Fölster, H.: Element loss on rain forest conversion in East Amazonia: comparison of balances of stores and fluxes, Biogeochemistry, 69, 63–82, https://doi.org/10.1023/B:BIOG.0000031040.38388.9b, 2004.

Komada, T., Anderson, M. R., and Dorfmeier, C. L.: Carbonate removal from coastal sediments for the determination of organic carbon and its isotopic signatures, δ13C and Δ14C: comparison of fumigation and direct acidification by hydrochloric acid, Limnology and Oceanography: Methods, 6, 254–262, https://doi.org/10.4319/lom.2008.6.254, _eprint: https://onlinelibrary.wiley.com/doi/pdf/10.4319/lom.2008.6.254, 2008.

Korchagin, J., Bortoluzzi, E. C., Moterle, D. F., Petry, C., and Caner, L.: Evidences of soil geochemistry and mineralogy changes caused by eucalyptus rhizosphere, CATENA, 175, 132–143, https://doi.org/10.1016/j.catena.2018.12.001, 2019.

Kulimushi, L. C., Choudhari, P., Mubalama, L. K., and Banswe, G. T.: GIS and remote sensing-based assessment of soil erosion risk using RUSLE model in South-Kivu province, eastern, Democratic Republic of Congo, Geomatics, Natural Hazards and Risk, 12, 961–987, https://doi.org/10.1080/19475705.2021.1906759, 2021.

Kurniawan, S., Corre, M. D., Matson, A. L., Schulte-Bisping, H., Utami, S. R., van Straaten, O., and Veldkamp, E.: Conversion of tropical forests to smallholder rubber and oil palm plantations impacts nutrient leaching losses and nutrient retention efficiency in highly weathered soils, Biogeosciences, 15, 5131–5154, https://doi.org/10.5194/bg-15-5131-2018, publisher: Copernicus GmbH, 2018.

Kögel-Knabner, I., Guggenberger, G., Kleber, M., Kandeler, E., Kalbitz, K., Scheu, S., Eusterhues, K., and Leinweber, P.: Organo-mineral associations in temperate soils: Integrating biology, mineralogy, and organic matter chemistry, Journal of Plant Nutrition and Soil Science, 171, 61–82, https://doi.org/10.1002/jpln.200700048, _eprint: https://onlinelibrary.wiley.com/doi/pdf/10.1002/jpln.200700048, 2008.

Laclau, J.-P., Ranger, J., Nzila, J. d. D., Bouillet, J.-P., and Deleporte, P.: Nutrient cycling in a clonal stand of *Eucalyptus* and an adjacent savanna ecosystem in Congo: 2. Chemical composition of soil solutions, Forest Ecology and Management, 180, 527–544, https://doi.org/10.1016/S0378-1127(02)00645-X, 2003.

Laclau, J.-P., Ranger, J., Deleporte, P., Nouvellon, Y., Saint-André, L., Marlet, S., and Bouillet, J.-P.: Nutrient cycling in a clonal stand of *Eucalyptus* and an adjacent savanna ecosystem in Congo: 3. Input–output budgets and consequences for the sustainability of the plantations, Forest Ecology and Management, 210, 375–391, https://doi.org/10.1016/j.foreco.2005.02.028, 2005.

Laganière, J., Angers, D. A., and Paré, D.: Carbon accumulation in agricultural soils after afforestation: a meta-analysis, Global Change Biology, 16, 439–453, https://doi.org/10.1111/j.1365-2486.2009.01930.x, _eprint: https://onlinelibrary.wiley.com/doi/pdf/10.1111/j.1365-2486.2009.01930.x, 2010.

Laghmouch, M., Buzera, C., Ilombe Mawe, G., Bamulezi, G., Nakito, E., Mugisho Bachinyaga, J., Birenjira, E., Wazi, N. R., and Nzolang, C.: Laghmouch M ., Kalikone, C., Ilombe G., Ganza G., Safari E., Bachinyaga J., Mugisho E., , Waz i N.,Nzolang C., Delvaux D., Dewaele S ., Fernandez M ., Mees F., Nimpagaritse G., Tack L. & Kervyn F. Carte géologique du Kivu au 1/500 000 (RD. CONGO). Musée Royal de l'Afrique Centrale, Tervuren. ISBN: 9789492669438, 2018.

Lal, R.: Restoring Soil Quality to Mitigate Soil Degradation, Sustainability, 7, 5875–5895, https://doi.org/10.3390/su7055875, number: 5 Publisher: Multidisciplinary Digital Publishing Institute, 2015.

Lambin, E. F., Turner, B. L., Geist, H. J., Agbola, S. B., Angelsen, A., Bruce, J. W., Coomes, O. T., Dirzo, R., Fischer, G., Folke, C., George, P. S., Homewood, K., Imbernon, J., Leemans, R., Li, X., Moran, E. F., Mortimore, M., Ramakrishnan, P. S., Richards, J. F., Skånes, H., Steffen, W., Stone, G. D., Svedin, U., Veldkamp, T. A., Vogel, C., and Xu, J.: The causes of land-use and land-cover change: moving beyond the myths, Global Environmental Change, 11, 261–269, https://doi.org/10.1016/S0959-3780(01)00007-3, 2001.

Lavallee, J. M., Soong, J. L., and Cotrufo, M. F.: Conceptualizing soil organic matter into particulate and mineral-associated forms to address global change in the 21st century, Global Change Biology, 26, 261–273, https://doi.org/10.1111/gcb.14859, _eprint: https://onlinelibrary.wiley.com/doi/pdf/10.1111/gcb.14859, 2020.

Lee, S. H., Dahali, R., Nik Hashim, N. H., Kusin, M., Mahmud, S. Z., Kamarudin, N., Abdul Jalil, A. M., and Lubis, M. A. R.: Eucalyptus Plantation Worldwide, Its Hybridization and Cloning Development, in: Eucalyptus: Engineered Wood Products and Other Applications, edited by Lee, S. H., Lum, W. C., Antov, P., Krišťák, , Rahandi Lubis, M. A., and Fatriasari, W., pp. 1–15, Springer Nature, Singapore, ISBN 978-981-9979-19-6, https://doi.org/10.1007/978-981-99-7919-6_1, 2024.

Leite, F. P., Silva, I. R., Novais, R. F., Barros, N. F. d., and Neves, J. C. L.: Alterations of soil chemical properties by eucalyptus cultivation in five regions in the Rio Doce Valley, Revista Brasileira de Ciência do Solo, 34, 821–831, https://doi.org/10.1590/S0100-06832010000300024, publisher: Sociedade Brasileira de Ciência do Solo, 2010.

Lejeune, G., Ansay, F., Van Geit, M., and Lusenge, T.: ECOmakala :répondre à la demande énergétique pour protéger les forêts du Parc National des Virunga au Nord-Kivu (RDC) et lutter contre la pauvreté, Tech. rep., World Wide Fund for Nature, Bruxelles, Belgium, 2013.

Lemenih, M., Olsson, M., and Karltun, E.: Comparison of soil attributes under *Cupressus lusitanica* and *Eucalyptus saligna* established on abandoned farmlands with continuously cropped farmlands and natural forest in Ethiopia, Forest Ecology and Management, 195, 57–67, https://doi.org/10.1016/j.foreco.2004.02.055, 2004.

Lewis, L. A. and Nyamulinda, V.: The critical role of human activities in land degradation in Rwanda, Land Degradation & Development, 7, 47–55, https://doi.org/10.1002/(SICI)1099-145X(199603)7:1<47::AID-LDR213>3.0.CO;2-M, _eprint: https://onlinelibrary.wiley.com/doi/pdf/10.1002/%28SICI%291099-145X%28199603%297%3A1%3C47%3A%3AAID-LDR213%3E3.0.CO%3B2-M, 1996.

Lima, A. M. N., Silva, I. R., Neves, J. C. L., Novais, R. F., Barros, N. F., Mendonça, E. S., Smyth, T. J., Moreira, M. S., and Leite, F. P.:
870   Soil organic carbon dynamics following afforestation of degraded pastures with eucalyptus in southeastern Brazil, Forest Ecology and
       Management, 235, 219–231, https://doi.org/10.1016/j.foreco.2006.08.331, 2006.

Link, K., Koehn, D., Barth, M. G., Tiberindwa, J. V., Barifaijo, E., Aanyu, K., and Foley, S. F.: Continuous cratonic crust between the Congo
       and Tanzania blocks in western Uganda, International Journal of Earth Sciences, 99, 1559–1573, https://doi.org/10.1007/s00531-010-
       0548-8, 2010.

875 López-Ulloa, M., Veldkamp, E., and de Koning, G. H. J.: Soil Carbon Stabilization in Converted Tropical Pastures and Forests
       Depends on Soil Type, Soil Science Society of America Journal, 69, 1110–1117, https://doi.org/10.2136/sssaj2004.0353, _eprint:
       https://onlinelibrary.wiley.com/doi/pdf/10.2136/sssaj2004.0353, 2005.

Majaliwa, J. G. M., Twongyirwe, R., Nyenje, R., Oluka, M., Ongom, B., Sirike, J., Mfitumukiza, D., Azanga, E., Natumanya, R., Mwerera,
       R., and Barasa, B.: The Effect of Land Cover Change on Soil Properties around Kibale National Park in South Western Uganda, Applied
880   and Environmental Soil Science, 2010, e185 689, https://doi.org/10.1155/2010/185689, publisher: Hindawi, 2010.

Maki Mateso, J.-C., Bielders, C. L., Monsieurs, E., Depicker, A., Smets, B., Tambala, T., Bagalwa Mateso, L., and Dewitte, O.: Characteristics
       and causes of natural and human-induced landslides in a tropical mountainous region: the rift flank west of Lake Kivu (Democratic
       Republic of the Congo), Natural Hazards and Earth System Sciences, 23, 643–666, https://doi.org/10.5194/nhess-23-643-2023, publisher:
       Copernicus GmbH, 2023.

885 Mallen-Cooper, M., Atkinson, J., Xirocostas, Z. A., Wijas, B., Chiarenza, G. M., Dadzie, F. A., and Eldridge, D. J.: Global synthesis reveals
       strong multifaceted effects of eucalypts on soils, Global Ecology and Biogeography, 31, 1667–1678, https://doi.org/10.1111/geb.13522,
       _eprint: https://onlinelibrary.wiley.com/doi/pdf/10.1111/geb.13522, 2022.

Markewitz, D., Davidson, E., Moutinho, P., and Nepstad, D.: Nutrient Loss and Redistribution After Forest Clearing
       on a Highly Weathered Soil in Amazonia, Ecological Applications, 14, 177–199, https://doi.org/10.1890/01-6016, _eprint:
890   https://onlinelibrary.wiley.com/doi/pdf/10.1890/01-6016, 2004.

Marín-Spiotta, E. and Sharma, S.: Carbon storage in successional and plantation forest soils: a tropical analysis, Global Ecology and Biogeog-
       raphy, 22, 105–117, https://doi.org/10.1111/j.1466-8238.2012.00788.x, _eprint: https://onlinelibrary.wiley.com/doi/pdf/10.1111/j.1466-
       8238.2012.00788.x, 2013.

May-Tobin, C., Boucher, D., Elias, P., Lininger, K., Roquemore, S., and Saxon, E.: Wood for Fuel, Tech. rep., Union of Concerned Scientists,
895   https://www.jstor.org/stable/resrep00075.14, 2011.

McLean, E. O.: Aluminum, in: Methods of Soil Analysis, pp. 978–998, John Wiley & Sons, Ltd, ISBN 978-0-89118-204-7,
       https://doi.org/10.2134/agronmonogr9.2.c16, section: 67 _eprint: https://onlinelibrary.wiley.com/doi/pdf/10.2134/agronmonogr9.2.c16,
       1965.

Melkebeke, S. V.: Dissimilar coffee frontiers : mobilizing labor and land in the lake kivu region, congo and rwanda (1918-1960/62), in:
900   Dissimilar coffee frontiers : mobilizing labor and land in the lake kivu region, congo and rwanda (1918-1960/62), African history ; 9,
       BRILL, Leiden, Netherlands ;, ISBN 90-04-42849-6, 2020.

Mikutta, R. and Kaiser, K.: Organic matter bound to mineral surfaces: Resistance to chemical and biological oxidation, Soil Biology and
       Biochemistry, 43, 1738–1741, https://doi.org/10.1016/j.soilbio.2011.04.012, 2011.

Mizota, C. and Reeuwijk, L. P. v.: Clay mineralogy and chemistry of soils formed in volcanic material in diverse climatic regions., Clay
905   mineralogy and chemistry of soils formed in volcanic material in diverse climatic regions., https://www.cabdirect.org/cabdirect/abstract/
       19901941362, 1989.

Moebius-Clune, B. N., van Es, H. M., Idowu, O. J., Schindelbeck, R. R., Kimetu, J. M., Ngoze, S., Lehmann, J., and Kinyangi, J. M.: Long-term soil quality degradation along a cultivation chronosequence in western Kenya, Agriculture, Ecosystems & Environment, 141, 86–99, https://doi.org/10.1016/j.agee.2011.02.018, 2011.

910 Muchena, F. N., Onduru, D. D., Gachini, G. N., and de Jager, A.: Turning the tides of soil degradation in Africa: capturing the reality and exploring opportunities, Land Use Policy, 22, 23–31, https://doi.org/10.1016/j.landusepol.2003.07.001, 2005.

Mutegeza Mushitwala, D.: Rapport bi-annuel 2018–2019, Tech. rep., Inspection Provinciale De l'agriculture du Sud-Kivu, South Kivu, Democratic Republic of Congo, 2020.

Namirembe, S., Piikki, K., Sommer, R., Söderström, M., Tessema, B., and Nyawira, S.: Soil organic carbon in agricultural systems of six

915 countries in East Africa – a literature review of status and carbon sequestration potential, South African Journal of Plant and Soil, 37, 35–49, https://doi.org/10.1080/02571862.2019.1640296, 2020.

Nanzyo, M., Dahlgren, R., and Shoji, S.: Chapter 6 Chemical Characteristics of Volcanic Ash Soils, in: Developments in Soil Science, edited by Shoji, S., Nanzyo, M., and Dahlgren, R., vol. 21 of *Volcanic Ash Soils*, pp. 145–187, Elsevier, https://doi.org/10.1016/S0166-2481(08)70267-8, 1993.

920 Nepstad, D. C., de Carvalho, C. R., Davidson, E. A., Jipp, P. H., Lefebvre, P. A., Negreiros, G. H., da Silva, E. D., Stone, T. A., Trumbore, S. E., and Vieira, S.: The role of deep roots in the hydrological and carbon cycles of Amazonian forests and pastures, Nature, 372, 666–669, https://doi.org/10.1038/372666a0, number: 6507 Publisher: Nature Publishing Group, 1994.

Newbury, D. S.: Kings and clans : Ijwi island and the lake kivu rift, 1780-1840, in: Kings and clans ijwi island and the lake kivu rift, 1780-1840, WISEdition, University of Wisconsin Press, Madison (Wis.) [etc, ISBN 0-299-12894-6, 2010.

925 Ng, W., Minasny, B., Jeon, S. H., and McBratney, A.: Mid-infrared spectroscopy for accurate measurement of an extensive set of soil properties for assessing soil functions, Soil Security, 6, 100 043, https://doi.org/10.1016/j.soisec.2022.100043, 2022.

Ngoze, S., Riha, S., Lehmann, J., Verchot, L., Kinyangi, J., Mbugua, D., and Pell, A.: Nutrient constraints to tropical agroecosystem productivity in long-term degrading soils, Global Change Biology, 14, 2810–2822, https://doi.org/10.1111/j.1365-2486.2008.01698.x, _eprint: https://onlinelibrary.wiley.com/doi/pdf/10.1111/j.1365-2486.2008.01698.x, 2008.

930 Nye, P. H. and Greenland, D. J.: Changes in the soil after clearing tropical forest, Plant and Soil, 21, 101–112, https://doi.org/10.1007/BF01373877, 1964.

Odeh, I. O. A., Todd, A. J., and Triantafilis, J.: SPATIAL PREDICTION OF SOIL PARTICLE-SIZE FRACTIONS AS COMPOSITIONAL DATA, Soil Science, 168, 501, https://doi.org/10.1097/01.ss.0000080335.10341.23, 2003.

Paul, S., Flessa, H., Veldkamp, E., and López-Ulloa, M.: Stabilization of recent soil carbon in the humid tropics following land use changes:

935 evidence from aggregate fractionation and stable isotope analyses, Biogeochemistry, 87, 247–263, https://doi.org/10.1007/s10533-008-9182-y, 2008.

Pauwels, J. M., Van Ranst, E., and Verloo, M.: Manuel de laboratoire de pédologie : méthodes d'analyse de sols et de plantes, équipement, gestion de stocks de verrerie et de produits chimiques, no. 28 in AGCD. Publications agricoles, Centre universitaire de Dschang. Département des sciences du sol, Yaoundé, 1992.

940 Posit team: RStudio: Integrated Development Environment for R, Tech. rep., Posit Software, PBC, Boston, MA, http://www.posit.co/, 2023.

Pouclet, A. and Bram, K.: Nyiragongo and Nyamuragira: a review of volcanic activity in the Kivu rift, western branch of the East African Rift System, Bulletin of Volcanology, 83, 10, https://doi.org/10.1007/s00445-021-01435-6, 2021.

Pouclet, A., Bellon, H., and Bram, K.: The Cenozoic volcanism in the Kivu rift: Assessment of the tectonic setting, geochemistry, and geochronology of the volcanic activity in the South-Kivu and Virunga regions, Journal of African Earth Sciences, 121, 219–246, https://doi.org/10.1016/j.jafrearsci.2016.05.026, 2016.

Powers, J. S., Corre, M. D., Twine, T. E., and Veldkamp, E.: Geographic bias of field observations of soil carbon stocks with tropical land-use changes precludes spatial extrapolation, Proceedings of the National Academy of Sciences, 108, 6318–6322, https://doi.org/10.1073/pnas.1016774108, publisher: Proceedings of the National Academy of Sciences, 2011.

Prosser, I. P., Hailes, K. J., Melville, M. D., Avery, R. P., and Slade, C. J.: A comparison of soil acidification and aluminum under Eucalyptus forest and unimproved pasture, Soil Research, 31, 245–254, https://doi.org/10.1071/sr9930245, publisher: CSIRO PUBLISHING, 1993.

Quesada, C. A., Paz, C., Oblitas Mendoza, E., Phillips, O. L., Saiz, G., and Lloyd, J.: Variations in soil chemical and physical properties explain basin-wide Amazon forest soil carbon concentrations, SOIL, 6, 53–88, https://doi.org/10.5194/soil-6-53-2020, publisher: Copernicus GmbH, 2020.

R Core Team: R: A Language and Environment for Statistical Computing, manual, R Foundation for Statistical Computing, Vienna, Austria, https://www.R-project.org/, 2023.

Ramirez-Lopez, L., Stevens, A., Orellano, C., Viscarra Rossel, R., Shen, Z., Wadoux, A., and Breure, T.: resemble: Regression and similarity evaluation for memory-based learning in spectral chemometrics. R package version 2.2.3, https://CRAN.R-project.org/package=resemble, 2024.

Ramirez-Lopez, L., Wadoux, A. M. J., Franceschini, M. H. D., Terra, F. S., Marques, K. P. P., Sayão, V. M., and Demattê, J. A. M.: Robust soil mapping at the farm scale with vis–NIR spectroscopy, European Journal of Soil Science, 70, 378–393, https://doi.org/10.1111/ejss.12752, 2019.

Rasmussen, C., Heckman, K., Wieder, W. R., Keiluweit, M., Lawrence, C. R., Berhe, A. A., Blankinship, J. C., Crow, S. E., Druhan, J. L., Hicks Pries, C. E., Marin-Spiotta, E., Plante, A. F., Schädel, C., Schimel, J. P., Sierra, C. A., Thompson, A., and Wagai, R.: Beyond clay: towards an improved set of variables for predicting soil organic matter content, Biogeochemistry, 137, 297–306, https://doi.org/10.1007/s10533-018-0424-3, 2018.

Reichenbach, M., Fiener, P., Garland, G., Griepentrog, M., Six, J., and Doetterl, S.: The role of geochemistry in organic carbon stabilization against microbial decomposition in tropical rainforest soils, SOIL, 7, 453–475, https://doi.org/10.5194/soil-7-453-2021, publisher: Copernicus GmbH, 2021.

Reichenbach, M., Fiener, P., Hoyt, A., Trumbore, S., Six, J., and Doetterl, S.: Soil carbon stocks in stable tropical landforms are dominated by geochemical controls and not by land use, Global Change Biology, 29, 2591–2607, https://doi.org/10.1111/gcb.16622, _eprint: https://onlinelibrary.wiley.com/doi/pdf/10.1111/gcb.16622, 2023.

Roose, E. and Barthès, B.: Organic matter management for soil conservation and productivity restoration in Africa: a contribution from Francophone research, Nutrient Cycling in Agroecosystems, 61, 159–170, https://doi.org/10.1023/A:1013349731671, 2001.

Rudel, T. K., Defries, R., Asner, G. P., and Laurance, W. F.: Changing Drivers of Deforestation and New Opportunities for Conservation, Conservation Biology, 23, 1396–1405, https://doi.org/10.1111/j.1523-1739.2009.01332.x, _eprint: https://onlinelibrary.wiley.com/doi/pdf/10.1111/j.1523-1739.2009.01332.x, 2009.

Ruff, M., Wacker, L., Gäggeler, H. W., Suter, M., Synal, H.-A., and Szidat, S.: A Gas Ion Source for Radiocarbon Measurements at 200 kV, Radiocarbon, 49, 307–314, https://doi.org/10.1017/S0033822200042235, 2007.

Sanchez, P. A. and Logan, T. J.: Myths and Science about the Chemistry and Fertility of Soils in the Tropics, in: Myths and Science of
Soils of the Tropics, pp. 35–46, John Wiley & Sons, Ltd, ISBN 978-0-89118-924-4, https://doi.org/10.2136/sssaspecpub29.c3, section: 3
_eprint: https://onlinelibrary.wiley.com/doi/pdf/10.2136/sssaspecpub29.c3, 1992.

Sanderman, J., Savage, K., and Dangal, S. R.: Mid-infrared spectroscopy for prediction of soil health indicators in the United States, Soil
Science Society of America Journal, 84, 251–261, https://doi.org/10.1002/saj2.20009, 2020.

Six, J., Feller, C., Denef, K., Ogle, S. M., De Moraes, J. C., and Albrecht, A.: Soil organic matter, biota and aggregation in temperateand
tropical soils - Effects of no-tillage, Agronomie, 22, 755–775, https://doi.org/10.1051/agro:2002043, 2002.

Soares, M. R. and Alleoni, L. R. F.: Contribution of Soil Organic Carbon to the Ion Exchange Capacity of Tropical Soils, Jour-
nal of Sustainable Agriculture, 32, 439–462, https://doi.org/10.1080/10440040802257348, publisher: Taylor & Francis _eprint:
https://doi.org/10.1080/10440040802257348, 2008.

Souza, I. F., Almeida, L. F. J., Jesus, G. L., Kleber, M., and Silva, I. R.: The mechanisms of organic carbon protection
and dynamics of C-saturation in Oxisols vary with particle-size distribution, European Journal of Soil Science, 68, 726–739,
https://doi.org/10.1111/ejss.12463, _eprint: https://onlinelibrary.wiley.com/doi/pdf/10.1111/ejss.12463, 2017.

Sparks, D. L., Singh, B., and Siebecker, M. G.: Environmental Soil Chemistry, Elsevier, ISBN 978-0-443-14035-8, google-Books-ID: GOq-
jEAAAQBAJ, 2022.

Stallard, R. F.: Terrestrial sedimentation and the carbon cycle: Coupling weathering and erosion to carbon burial, Global Biogeochemical
Cycles, 12, 231–257, https://doi.org/10.1029/98GB00741, _eprint: https://onlinelibrary.wiley.com/doi/pdf/10.1029/98GB00741, 1998.

Stevens, A. and Ramirez-Lopez, L.: An introduction to the prospectr package. R package version 0.2.7, https://github.com/l-ramirez-lopez/
prospectr, 2024.

Stoner, S., Trumbore, S. E., González-Pérez, J. A., Schrumpf, M., Sierra, C. A., Hoyt, A. M., Chadwick, O., and Doetterl, S.: Relating min-
eral–organic matter stabilization mechanisms to carbon quality and age distributions using ramped thermal analysis, Philosophical Trans-
actions of the Royal Society A: Mathematical, Physical and Engineering Sciences, 381, 20230 139, https://doi.org/10.1098/rsta.2023.0139,
publisher: Royal Society, 2023.

Stucki, J. W., Goodman, B. A., and Schwertmann, U., eds.: Iron in Soils and Clay Minerals, Springer Netherlands, Dordrecht, ISBN 978-94-
010-8278-5 978-94-009-4007-9, https://doi.org/10.1007/978-94-009-4007-9, 1987.

Stuiver, M. and Polach, H. A.: Discussion Reporting of 14C Data, Radiocarbon, 19, 355–363, https://doi.org/10.1017/S0033822200003672,
1977.

Summerauer, L., Baumann, P., Ramirez-Lopez, L., Barthel, M., Bauters, M., Bukombe, B., Reichenbach, M., Boeckx, P., Kearsley, E.,
Van Oost, K., Vanlauwe, B., Chiragaga, D., Heri-Kazi, A. B., Moonen, P., Sila, A., Shepherd, K., Bazirake Mujinya, B., Van Ranst, E.,
Baert, G., Doetterl, S., and Six, J.: The central African soil spectral library: a new soil infrared repository and a geographical prediction
analysis, SOIL, 7, 693–715, https://doi.org/10.5194/soil-7-693-2021, publisher: Copernicus GmbH, 2021.

Tererai, F., Gaertner, M., Jacobs, S. M., and Richardson, D. M.: Eucalyptus Camaldulensis Invasion in Riparian Zones Reveals Few Sig-
nificant Effects on Soil Physico-Chemical Properties, River Research and Applications, 31, 590–601, https://doi.org/10.1002/rra.2762,
_eprint: https://onlinelibrary.wiley.com/doi/pdf/10.1002/rra.2762, 2015.

Tisdall, J. M. and Oades, J. M.: Organic matter and water-stable aggregates in soils, Journal of Soil Science, 33, 141–
163, https://doi.org/10.1111/j.1365-2389.1982.tb01755.x, _eprint: https://onlinelibrary.wiley.com/doi/pdf/10.1111/j.1365-
2389.1982.tb01755.x, 1982.

Tugel, A. J., Herrick, J. E., Brown, J. R., Mausbach, M. J., Puckett, W., and Hipple, K.: Soil Change, Soil Survey, and Natural Resources Decision Making, Soil Science Society of America Journal, 69, 738–747, https://doi.org/10.2136/sssaj2004.0163, _eprint: https://onlinelibrary.wiley.com/doi/pdf/10.2136/sssaj2004.0163, 2005.

Tully, K., Sullivan, C., Weil, R., and Sanchez, P.: The State of Soil Degradation in Sub-Saharan Africa: Baselines, Trajectories, and Solutions, Sustainability, 7, 6523–6552, https://doi.org/10.3390/su7066523, number: 6 Publisher: Multidisciplinary Digital Publishing Institute, 2015.

Tyukavina, A., Hansen, M. C., Potapov, P., Parker, D., Okpa, C., Stehman, S. V., Kommareddy, I., and Turubanova, S.: Congo Basin forest loss dominated by increasing smallholder clearing, Science Advances, 4, 1–12, https://doi.org/10.1126/sciadv.aat2993, 2018.

Van Oost, K. and Six, J.: Reconciling the paradox of soil organic carbon erosion by water, Biogeosciences, 20, 635–646, https://doi.org/10.5194/bg-20-635-2023, publisher: Copernicus GmbH, 2023.

Van Oost, K., Verstraeten, G., Doetterl, S., Notebaert, B., Wiaux, F., Broothaerts, N., and Six, J.: Legacy of human-induced C erosion and burial on soil–atmosphere C exchange, Proceedings of the National Academy of Sciences, 109, 19 492–19 497, https://doi.org/10.1073/pnas.1211162109, publisher: Proceedings of the National Academy of Sciences, 2012.

van Straaten, O., Corre, M. D., Wolf, K., Tchienkoua, M., Cuellar, E., Matthews, R. B., and Veldkamp, E.: Conversion of lowland tropical forests to tree cash crop plantations loses up to one-half of stored soil organic carbon, Proceedings of the National Academy of Sciences, 112, 9956–9960, https://doi.org/10.1073/pnas.1504628112, publisher: Proceedings of the National Academy of Sciences, 2015.

Vanacker, V., Ameijeiras-Mariño, Y., Schoonejans, J., Cornélis, J.-T., Minella, J. P. G., Lamouline, F., Vermeire, M.-L., Campforts, B., Robinet, J., Van de Broek, M., Delmelle, P., and Opfergelt, S.: Land use impacts on soil erosion and rejuvenation in Southern Brazil, CATENA, 178, 256–266, https://doi.org/10.1016/j.catena.2019.03.024, 2019.

Veldkamp, E., Schmidt, M., Powers, J. S., and Corre, M. D.: Deforestation and reforestation impacts on soils in the tropics, Nature Reviews Earth & Environment, 1, 590–605, https://doi.org/10.1038/s43017-020-0091-5, 2020.

Vinogradov, V. I.: C ^{13}/C ^{12} and O ^{18}/O ^{16} ratios and C ^{14} concentration in carbonatites of the Kaliango volcano (East Africa), International Geology Review, 22, 51–57, https://doi.org/10.1080/00206818209466862, 1980.

Vitousek, P., Chadwick, O., Matson, P., Allison, S., Derry, L., Kettley, L., Luers, A., Mecking, E., Monastra, V., and Porder, S.: Erosion and the Rejuvenation of Weathering-derived Nutrient Supply in an Old Tropical Landscape, Ecosystems, 6, 762–772, https://doi.org/10.1007/s10021-003-0199-8, 2003.

Vollset, S. E., Goren, E., Yuan, C.-W., Cao, J., Smith, A. E., Hsiao, T., Bisignano, C., Azhar, G. S., Castro, E., Chalek, J., Dolgert, A. J., Frank, T., Fukutaki, K., Hay, S. I., Lozano, R., Mokdad, A. H., Nandakumar, V., Pierce, M., Pletcher, M., Robalik, T., Steuben, K. M., Wunrow, H. Y., Zlavog, B. S., and Murray, C. J. L.: Fertility, mortality, migration, and population scenarios for 195 countries and territories from 2017 to 2100: a forecasting analysis for the Global Burden of Disease Study, The Lancet, 396, 1285–1306, https://doi.org/10.1016/S0140-6736(20)30677-2, 2020.

Vågen, T.-G., Winowiecki, L. A., Desta, L., Tondoh, E. J., Weullow, E., Shepherd, K., and Sila, A.: Mid-Infrared Spectra (MIRS) from ICRAF Soil and Plant Spectroscopy Laboratory: Africa Soil Information Service (AfSIS) Phase I 2009-2013, World Agroforestry - Research Data Repository, V1, Last access: 2020-08-10, https://doi.org/10.34725/DVN/QXCWP1, 2020.

Vågen, T.-G., Winowiecki, L. A., Desta, L., Tondoh, J., Weullow, E., Shepherd, K., Sila, A., Dunham, S. J., Hernández-Allica, J., Carter, J., and McGrath, S. P.: Wet chemistry data for a subset of AfSIS: Phase I archived soil samples, https://doi.org/10.34725/DVN/66BFOB, 2022.

Wambede, N. M., Joyfred, A., and Remigio, T.: Soil Loss under Different Cropping Systems in Highlands of Uganda, Universal Journal of Agricultural Research, 4, 217–229, https://doi.org/10.13189/ujar.2016.040601, publisher: Horizon Research Publishing, 2016.

1055 Wasige, J. E., Groen, T. A., Rwamukwaya, B. M., Tumwesigye, W., Smaling, E. M. A., and Jetten, V.: Contemporary land use/land cover types determine soil organic carbon stocks in south-west Rwanda, Nutrient Cycling in Agroecosystems, 100, 19–33, https://doi.org/10.1007/s10705-014-9623-z, 2014.

Wells, J. J., Stringer, L. C., Woodhead, A. J., and Wandrag, E. M.: Towards a holistic understanding of non-native tree impacts on ecosystem services: A review of Acacia, Eucalyptus and Pinus in Africa, Ecosystem Services, 60, 101 511,
1060 https://doi.org/10.1016/j.ecoser.2023.101511, 2023.

Wickham, H.: ggplot2: Elegant Graphics for Data Analysis, https://ggplot2.tidyverse.org, 2016.

Wieder, W. R., Grandy, A. S., Kallenbach, C. M., Taylor, P. G., and Bonan, G. B.: Representing life in the Earth system with soil microbial functional traits in the MIMICS model, Geoscientific Model Development, 8, 1789–1808, https://doi.org/10.5194/gmd-8-1789-2015, publisher: Copernicus GmbH, 2015.

1065 Wilken, F., Fiener, P., Ketterer, M., Meusburger, K., Muhindo, D. I., van Oost, K., and Doetterl, S.: Assessing soil redistribution of forest and cropland sites in wet tropical Africa using $^{239+240}$Pu fallout radionuclides, SOIL, 7, 399–414, https://doi.org/10.5194/soil-7-399-2021, publisher: Copernicus GmbH, 2021.

WorldPop: The spatial distribution of population density in 2020, Democratic Republic of Congo, https://doi.org/10.5258/SOTON/WP00674, 2020.

1070 Wu, S., Konhauser, K. O., Chen, B., and Huang, L.: "Reactive Mineral Sink" drives soil organic matter dynamics and stabilization, npj Materials Sustainability, 1, 3, https://doi.org/10.1038/s44296-023-00003-7, 2023.

Xiong, M., Sun, R., and Chen, L.: A global comparison of soil erosion associated with land use and climate type, Geoderma, 343, 31–39, https://doi.org/10.1016/j.geoderma.2019.02.013, 2019.

Yavitt, J. B.: Nutrient Dynamics of Soil Derived from Different Parent Material on Barro Colorado Island, Panama1, Biotropica, 32, 198–207,
1075 https://doi.org/10.1111/j.1744-7429.2000.tb00462.x, 2000.

Zhang, D., Zhang, J., Yang, W., and Wu, F.: Effects of afforestation with Eucalyptus grandis on soil physicochemical and microbiological properties, Soil Research, 50, 167–176, https://doi.org/10.1071/SR11104, publisher: CSIRO PUBLISHING, 2012.